Solvatochromism as an efficient tool to study N,N-dimethylamino- and cyano substituted π-conjugated molecules with an intramolecular charge-transfer absorption

Filip Bureš, Oldřich Pytela, Milan Kivala, François Diederich

Journal of Physical Organic Chemistry

Solvatochromism as an efficient tool to study N,N-dimethylamino- and cyano substituted π-conjugated molecules with an intramolecular charge-transfer absorption

Journal:	*Journal of Physical Organic Chemistry*
Manuscript ID:	POC-10-0058.R1
Wiley - Manuscript type:	Research Article
Date Submitted by the Author:	12-Apr-2010
Complete List of Authors:	Bureš, Filip; University of Pardubice, Faculty of Chemical Technology, Institute of Organic Chemistry and Technology Pytela, Oldřich; University of Pardubice, Faculty of Chemical Technology, Institute of Organic Chemistry and Technology Kivala, Milan; ETH-Zurich, Laboratorium fur Organische Chemie Diederich, François; ETH-Zûrich, Laboratorium fûr Organische Chemie
Keywords:	solvent effects, solvatochromism, UV/Vis spectroscopy, donor-acceptor system, chromophore

Solvatochromism as an efficient tool to study *N,N*-dimethylamino- and cyano-substituted π-conjugated molecules with an intramolecular charge-transfer absorption

Filip Bureš,* [a] Oldřich Pytela* [a], Milan Kivala,[b] and François Diederich[b]

[a]*Institute of Organic Chemistry and Technology, Faculty of Chemical Technology, University of Pardubice, Studentská 573, CZ-532 10, Pardubice, Czech Republic, E-mail: filip.bures@upce.cz, oldrich.pytela@upce.cz*

[b]*Laboratorium fűr Organische Chemie, ETH-Zűrich, Hönggerberg, HCI, 8093, Zűrich, Switzerland, E-mail: diederich@org.chem.ethz.ch*

Keywords: solvent effects, solvatochromism, UV/Vis spectroscopy, donor-acceptor system

A representative data set has been gained by the measurement of the electronic absorption spectra of twelve systematically selected push-pull systems with an intramolecular charge-transfer (CT) absorption and the general structure D-π-A (D = donor, A = acceptor) featuring electron-withdrawing CN groups, electron-donating $N(CH_3)_2$ groups, and various π-conjugated backbones in 32 solvents with different polarity. The longest-wavelength absorption maxima λ_{max} and the corresponding wavenumbers $\tilde{\nu}_{max}$ were evaluated from the UV/Vis spectra measured in 32 well-selected solvents. The D-π-A push-pull systems were further characterized by quantum-chemical quantities and simple structural parameters. Structure-solvatochromism relationships were evaluated by multidimensional statistic methods. Whereas solvent polarizability and solvent cavity size proved to be the most important factors affecting the position of λ_{max}, the solvent polarity was less important. The most important characteristics of organic charge-transfer compounds are the energy of the LUMO, the permanent dipole moment, the COSMO (COnductor-like Screening MOdel) area, the COSMO volume, the number and ratio of *N,N*-dimethylamino and cyano groups, and eventually the number of triple bonds (π–linkers). A relation between the first-order polarizability α, the longest-wavelength absorption maxima λ_{max}, and the structural features

has also been found. The higher-order polarizabilities β and γ are not related to the observed solvatochromism.

INTRODUCTION

π-Conjugated organic molecules attract much attention due to their prospective application as efficient materials in organic electronics and optoelectronics.[1,2] A typical organic charge-transfer chromophore (D-π-A) consists of strong electron donors D (e.g. NR_2 or OR groups), strong electron acceptors A (e.g. NO_2 or CN groups), and a π-conjugated core featuring (hetero)aromatic rings and/or double or triple bonds.[3-5] Optical linear and nonlinear properties of such push-pull molecules depend on the polarizability of the electrons localized in π–bonding molecular orbitals.[6] Although the polarizability of a molecule is mainly given by its chemical structure, in particular by the length of the π-conjugated spacer and the electronic nature of the donors and acceptors attached,[7-9] it can also be affected by external factors such as strength of radiation, state of matter, and in solution also by the solvent used. However, a general description of external factors (solvent) affecting optical and nonlinear optical properties is more complex. In our previous investigation we have studied solvent effects on the electronic absorption spectra of donor-substituted 11,11,12,12-tetracyano-9,10-anthraquinodimethanes (TCAQs **10**–**12**, Figure 1).[10,11] Optical properties of these model charge-transfer (CT) solvatochromic indicators were investigated in 32 solvents of various nature. The resulting data were evaluated by means of theoretical models and (semi)empirical correlations determining the optical properties related to electron distribution and polarizability. The present work focuses on organic D-π-A molecules with *N*,*N*-dimethylanilino (DMA) groups as donors and cyano groups as acceptors featuring various π-conjugated spacers (Figure 1). Whereas the first class of molecules is represented by cyanoethynylethenes **1**–**3** (CEEs),[12-14] the second class consists of three donor-substituted 7,7,8,8-tetracyanoquinodimethane-based molecules **4**–**6** (TCNQ-based).[15] Molecules **7**–**9** represent donor-substituted 1,1,4,4-tetracyanobuta-1,3-dienes (TCBDs).[16-18] The compounds shown in Figure 1 were chosen according to their different molecular properties and geometries. The chosen set comprises planar (**1**–**3**) or nonplanar (others) molecules, centrosymmetric (**2**) or nearly centrosymmetric (**8**, **11**) compounds, quinoid (**4**–**6**) or fused quinoid (**10**–**12**) molecules, and molecules bearing CC triple bonds (**1**–**3**, **6**, and **9**) or 1,4-phenylene units as additional π–linkers and simultaneously a different number of DMA and cyano groups.

Figure 1

A goal of this study is to investigate the relationships between the structure of D-π-A organic molecules and their solvatochromic properties and to find fundamental structural characteristics and solvent properties that can be used for a quantitative description of these relations.

RESULTS AND DISCUSSION

Data and methods

The change in the UV/Vis spectra of compound **5** in the wavelength range from 400 to 900 nm as a function of solvent is illustrated in Figure 2 (for complete spectra see Figures 1SI–45SI in Supporting Information). The absence of possible solute aggregation and concomitant influence on the position of the absorption maxima was verified by measurements of the UV/Vis spectra for **1**–**9** in dichloromethane (see SI) where the Lambert–Beer law was fully obeyed. The values of the longest-wavelength absorption maxima λ_{max} measured in 32 representative solvents for compounds **1**–**9** are summarized in Table 1. The λ_{max} values of TCAQs **10**–**12** were taken from the previous work.[10] All of the λ_{max} values were converted for further evaluation into the wavenumbers $\tilde{\nu}_{max}$ having energy dimension. The CT character of the longest-wavelength absorption of compounds **1**–**9** was already confirmed by protonation/neutralization experiments.[10-18]

Figure 2

Table 1

The $\tilde{\nu}_{max}$ values were ordered in a matrix with 32 rows (solvents, objects) and 12 columns (solvatochromic indicators, properties). Several statistic methods were tested for the data treatment. However, the methods of exploratory analysis (EA), methods with latent variables

(principal component analysis PCA and factor analysis FA), and methods based on multiple linear regression (MLR) showed to be the most suitable.

The algorithm NIPAL[19] in Exner variation[20] was used for the calculation of the latent variables of the native matrix **X** in PCA. This algorithm involves modification of the coordinate origin for each column of the matrix of manifest variables during the calculation. The FA factors were calculated from the correlation matrix **R**, covariance matrix **C**, and matrix $\mathbf{X}^T\mathbf{X}$ using nonlinear regression according to the basic factor model. Thus, it was possible to efficiently analyze non-standardized data with the same scale but with different origin in this way. Depending on the used method, this calculation provided separate sets of score **T** and loadings matrixes **F**, which were further physico-chemically interpreted.

Beside the quantum-chemical quantities used for the description of molecule properties, the structural characteristics expressed as a number of present structural features were also successfully employed. This method is common in QSAR (quantitative structure-activity relationships). With respect to the number of indicators and possible multicollinearity, the maximum number of the explanatory variables was limited to three. Selection of the most suitable explanatory variables in the linear regression was performed by the calculation for all possible combinations of the proposed set of variables according to the minimal residual standard deviation. The regressions with the selected combination of the explanatory variables were tested by regression diagnostic (including t-test, F-test, assessing multicollinearity, residual analysis) for statistic validity. A similar principle was used for the selection of the most suitable explanatory variables characterizing the used solvents.

Exploratory data analysis

Exploratory analysis is a simple and efficient tool for primary data screening. A mutual comparison of the longest-wavelength absorption maxima λ_{max} of the intramolecular CT bands measured for compounds **1**–**9** in 32 different solvents (Table 1) through the polygon's size and shape is shown in Figure 3. It is obvious that compounds **4**, **5**, and **6** have the highest λ_{max} values. The cut in the upper part of polygon **4** was caused by the missing triethylamine value. The same solvent was indicated to be exceptional by the rising ray in the right upper part of the polygons **5** and **6** (remarkable also for other compounds). The observed high λ_{max} values for componds **4**–**6** were most probably caused by the quinoid partial structure (TCNQ) of the molecule. From the spectral point of view, the quinoid motive is a combination of two

carbonyls and two π-bonds in a mutual interaction. The spectral transitions are given by the local electron transitions on the "enedione" motive (so-called "quinoid transitions"). The substituents in the area of carbonyls or fused aromatic rings (see TCAQ's **10**–**12**) may show their own local electron transitions (e.g. benzoid transitions in the case of benzene rings). Thus, the interaction of "enedione" and "benzoid" moieties shows CT transitions accompanied by a bathochromic shift of λ_{max}. From the polygon sizes in Figure 3, it is obvious that CT transitions between the "enedione" moiety and the fused benzene rings in molecular structures **10**–**12** are considerably weaker compared to those of the TCNQ-based molecular structures **4**–**6**. This is presumably due to the electron inter-connection which can change the π-bond character of the "enedione" moiety.

Figure 3

The TCBD series of solvatochromic indicators **7**–**9** showed undoubtedly the least polygon's area. The main structural feature of these compounds is the buta-1,3-diene backbone with two appended terminal cyano groups in a non-coplanar arrangement with the donor DMA substituents at the positions 2 and 3 of the butadiene moiety.[17] The CT interaction between both parts is most probably not caused by the number of donors (one DMA in **7** and two DMAs in **8** and **9**) but rather by the spatial arrangements and the difference in the energies of the local electron transitions.

The polygon's shapes in Figure 3 evidence the differences between the λ_{max} values given by the various solvent effects. The polygons **3** and **7** have remarkable irregular shape. The histogram of the λ_{max} frequency distribution in dependence on λ_{max} clearly shows bimodal distribution of the λ_{max} values for these two indicators. The group of solvents with the lower λ_{max} values (indicator **3**) includes both HBD (hydrogen-bond donor) solvents (alcohols, formamide) and *non*-HBD solvents (dimethylsulfoxide or *N*,*N*-dimethylacetamide – one of the most polar solvents). For indicator **7**, this group of solvents is even extended to tetrahydrofuran(!), esters, ketones, nitrocompounds, etc. In other words, the afore-mentioned solvents "switch off" the intramolecular CT transition and the observed λ_{max} values correspond to a local π-π^* or n-π^* transitions of any molecule part (see also the Supporting Information). We can consider several reasons of such a "switch off" related either to the structure of the compound or to the solvent properties. The first reason is a disproportion

between the number of electron donating DMA groups (one) and the number of electron withdrawing cyano groups (three for **3** and four for **7**) in contrast to other molecules. The second structural reason is the localization of the well accessible cyano groups, as well as the LUMO, at the molecule terminus. Both of these reasons are related with an intramolecular hydrogen bond interaction between the terminal nitrogens of the cyano groups and acidic hydrogens of the HBD solvents or with an interaction between the LUMO of indicator and the lone pairs of the HBA solvents. For the solvent classification see ref.[21] Both of these effects change the LUMO properties of the solvatochromic indicators and, consequently, also the intramolecular interaction and character of the electron transition. Last but not least, the observed "switch off" can be caused by the solvent properties. The molecules of protic solvents are hydrogen bonded to each other and, therefore, the cavity surrounding the solute (indicator) is more rigid. Such a rigid cavity suppresses the effective electron reorganization in the transition from the ground to the excited state, which results in a hypsochromic shift. This effect can be observed selectively in dependence on the molecular structure of indicators.

A comparison of the experimental λ_{max} values measured in methanol with those quantum-chemically calculated (ZINDO-CI, methanol) seems to be interesting in this respect. Whereas the experimental λ_{max} values of all indicatores exceeded the calculated ones (e.g. indicator **4** – calculated 569.2 nm, found 669.5 nm; indicator **8** – calculated 378.4 nm, found 470 nm), the experimental and calculated λ_{max} values for **7** are quite similar (calculated 436.9 nm, found 443 nm).

Solvatochromism-structure relationships for D-π-A molecules

Factor analysis (FA) has been applied to evaluate a relation between solvatochromic indicators characterized by the $\tilde{\nu}_{max}$values in different solvents. The FA proved to be more suitable than PCA because the calculated factor loadings do not suffer from unicity of the particular columns. The factor loadings calculated by the decomposition of the correlation matrix **R**, covariance matrix **C**, and matrix $\mathbf{X}^T\mathbf{X}$ were significantly different. The performed analysis and several attempts of their interpretation showed that the $\tilde{\nu}_{max}$values themselves are crucial and depend on the coordinate origin as well as on the scale. Thus, the factor loadings calculated by the decomposition of the $\mathbf{X}^T\mathbf{X}$ matrix with two factors were used for interpretation of the structure-solvatochromism relationships.

Table 2

The calculated $\mathbf{f}_1$ and $\mathbf{f}_2$ loadings are summarized in Table 2. Relationships of points corresponding to the particular indicators **1**–**12** in the plane of $\mathbf{f}_1$ and $\mathbf{f}_2$ are shown in Figure 4. It can be clearly seen that indicators **3** and **7** are exceptional, which unambiguously corresponds with the results of the exploratory analysis (see above). In contrast to others, the TCNQ-based indicators **4**–**6** contain quinoid moieties and, therefore, their λ_{max} are shifted more bathochromically. The near location of **5** and **6** shows, that the acetylene linker in **6** has a small impact on the CT transition in such class of compounds. On the other hand, a replacement of hydrogen in **4** with an additional DMA donor (**5**) led to a bathochromic shift (see also the polygon expansion in Figure 3). The location of indicators **3** and **7** in the upper part confirm their unique, above-discussed properties.

Interpretation of the factor loadings $\mathbf{f}_1$ and $\mathbf{f}_2$ (Table 2) through the calculated and/or structural characteristics summarized in Table 3 provided a better insight into the structure-solvatochromism relationships. The following quantum-chemically calculated characteristics were used: (i) E_{HOMO} and E_{LUMO} energies; (ii) permanent dipole moment μ; (iii) COSMO (COnductor-like Screening MOdel) area; (iv) COSMO volume; (v) molecular dimensions MD1, MD2, and MD3, and (vi) their functions MD1×MD2, MD1×MD3, MD2×MD3, MD1×MD2×MD3, MD1/MD2, MD2/MD1, MD1/MD3, and MD3/MD1. As the characteristics describing structural features of the studied molecules were chosen: (i) number of DMA units n_{DMA}; (ii) number of cyano groups n_{CN}; (iii) number of triple bonds n_T; (iv) ratio n_{DMA}/n_{CN}; (v) ratio n_{CN}/n_{DMA}, and (vi) the indicator variables (0 not present, 1 present) – presence of quinoid arrangement i_{CH}, planarity i_{PL}, and centrosymmetry i_{CS}.

Table 3

The interpretation of the factor loadings $\mathbf{f}_1$ on the molecular structure of indicators was complicated by the values of **4**–**6**, that were in regression indicated as extremes. Hence, the obtained dependencies were represented by a connecting line between two clusters (**4**–**6** and others) and, therefore, the values of **4**–**6** were omitted from the further calculations and the new vector was marked as $\mathbf{f}_{1,-456}$. The strongest and statistically valid correlation can be described by equation (1)

$$\mathbf{f}_{1,\text{-}456} = (2.98\pm0.16)\ 10^{-3} + (5.56\pm0.78)\ 10^{-4}\ E_{\text{LUMO}} +$$
$$+ (1.53\pm0.52)\ 10^{-5}\ \mu\ - (1.91\pm0.27)\ 10^{-4}\ n_{\text{T}}\ , \qquad (1)$$
$$n = 9,\ s = 4.01\ 10^{-5},\ R = 0.961.$$

Equation (1) implies that the factor loadings value $\mathbf{f}_{1,\text{-}456}$ decreases with decreasing energy of the LUMO, decreasing permanent dipole moment μ, and with increasing number of triple bonds. The factor loadings $\mathbf{f}_1$ highly correlate with the $\tilde{\nu}_{max}$ values (for aprotic nonpolar solvents with R>0.95 and for dipolar protic solvents with R>0.8). Indicators with the smallest $\mathbf{f}_1$ have simultaneously the highest λ_{max} and vice versa (see Figure 3). In connection with equation (1) we can deduce, that the chomophores featuring a low LUMO energy, "suitable π-conjugated enlargers", and rather low permanent dipole moment (less "electron rigid" molecules) will possess the most bathochromically shifted λ_{max}.

In contrast to $\mathbf{f}_1$, the factor loadings $\mathbf{f}_2$ significantly correlate only with the $\tilde{\nu}_{max}$ values in protic solvents (R>0.6, positive correlation coefficient). This implies that $\mathbf{f}_2$ describes in particular the influence of such class of solvents (higher $\mathbf{f}_2$ values means also higher $\tilde{\nu}_{max}$). The anomalous effect of the protic solvents on the λ_{max} of **3** and **7** has been discussed before. A dependence of the factor loadings $\mathbf{f}_2$ on the structural characteristics of solvatochromic indicators provided a better insight into the problem. Thus, the dependence of the factor loadings $\mathbf{f}_2$ on the structural characteristics provided the strong and statistically valid equation (2)

$$\mathbf{f}_2 = -(1.16\pm0.52)\ 10^{-3} - (6.65\pm1.67)\ 10^{-7}\ \text{COSMO area} +$$
$$+ (1.71\pm0.55)\ 10^{-3}\ \text{COSMO area/COSMO volume}\ - (1.51\pm0.48)\ 10^{-4}\ i_{\text{PL}}, \qquad (2)$$
$$n = 12,\ s = 3.00\ 10^{-5},\ R = 0.941.$$

Equation (2) implies that the factor loadings $\mathbf{f}_2$, respectively $\tilde{\nu}_{max}$, decrease with increasing solvatable surface (COSMO area) of the molecule and decreasing ratio of the solvatable surface to the solvatable volume of the molecule (increasing "sphericity" of the solute). This trend is consistent for planar (i_{PL} = 1) as well as nonplanar (i_{PL} = 0) molecules. Based on these observations we can conclude that an additional effect of the solvent cavity lowering the longest-wavelength absorption maxima λ_{max} takes place in protic solvents, especially for small molecules (Figure 4, indicators **3** and **7**).

Solvatochromism-solvent properties relationships

Principal component analysis (PCA) was applied to evaluate solvent effects on the $\tilde{\nu}_{max}$ values for different D-π-A organic molecules as solvatochromic indicators. The latent variables **t** (columns of the matrix **T**) as characteristics of solvent effects were calculated from the native (non-standardized) matrix **X**. The PCA method has mainly been chosen because the information on solvent effects can be calculated by the methods based on the similarity principle (similar to the structure-solvatochromism relationships of D-π-A molecules). The first latent variable explains 55.7 %, the second 28.7 %, and the third 11.4 % of the data variability (95.8 % of the explained variability overall). It is obvious that, with respect to the experimental accuracy, the three latent variables described the total relevant variability. The first latent variable describes dominantly solvent effects on indicators **3** (communality h^2 = 0.825) and **7** (h^2 = 0.635), while the effect of other indicators is small (h^2 = 0.01 – 0.39). The reasons have already been discussed before. The second latent variable particularly comprises solvent effects on indicators **1**, **2**, **4**–**6**, and **8**, while the third variable describes the interaction with indicators **9**-**12**. The specific effect of protic and very polar solvents on the longest-wavelength absorption maxima λ_{max} accompanied by the data decomposition is significant to such a degree that the structure of the score matrix **T** is deformed. Hence, the columns corresponding to indicators **3** and **7** were excluded from the matrix **X** and the procedure was repeated. Now, the first latent variable explains 71.2 %, the second 14.4 %, and the third 10.2 % of the data variability (95.8 % of the explained variability overall). Thus, the first latent variable substantially describes the data variability. The variability described by the first three latent variables is similar to the previous case, however, their structure is different.

Interpretation of the latent variable vectors $\mathbf{t}_1$ and $\mathbf{t}_2$ has been accomplished through the (semi)empirical solvent parameters ($f(n^2)$,$f(\varepsilon_r)$, V_m, and δ_H).[10] The strongest and statistically valid correlation for vector $\mathbf{t}_1$ can be described by equation (3)

$$\mathbf{t}_1 = (6.96\pm0.01)\ 10^{-1} + (2.92\pm0.67)\ 10^{-4}\ V_m - (4.56\pm0.36)\ 10^{-1}\ (n^2-1)/(n^2+2) + \\ + (1.36\pm0.01)\ 10^{-1}\ 1/\varepsilon_r, \qquad (3)$$

$$n = 32,\ s = 6.53\ 10^{-3},\ R = 0.983.$$

Likewise, the strongest and valid dependence for $\mathbf{t}_2$ can be expressed by equation (4):

$$\mathbf{t}_2 = (7.90\pm9.43)10^{-1} + (2.38\pm0.60)\ 10^{-2}\ V_m - (1.81\pm0.30)\ 10^{1}\ (n^2-1)/(n^2+2) +$$

$$+ (3.93\pm0.60)\ 10^{-3}\ \delta_H^2, \qquad (4)$$

$$n = 32,\ s = 5.61\ 10^{-1},\ R = 0.850.$$

A joint interpretation of equations (3) and (4) implies that dominant solvent effects on the position of λ_{max} are, in descending order, solvent polarizability, solvent cavity size, and solvent polarity. According to the previous discussion,[10] increasing solvent polarizability and polarity shifts the longest-wavelength absorption maxima λ_{max} bathochromically, while the solvent cavity size has the opposite effect (hypsochromic shift).

Solvatochromism-polarizability relationships

First- (α), second- (β), and third-order (γ) polarizabilities of indicators **1**–**12** calculated by MOPAC2009 are summarized in Table 3. The afore-mentioned structural characteristics and the $\tilde{\nu}_{max}$ values in all 32 solvents were used for the interpretation of the calculated polarizabilities. A statistically significant dependence has been found only for the first-order polarizability α. This implies that the higher-order polarizabilities are not related to solvatochromism.

A simple and statistically valid interpretation of the first-order polarizability α is given by equation (5):

$$\alpha = (9.83\pm0.85)\ 10^{-30} - (2.46\pm0.39)\ 10^{-27}\ \tilde{\nu}_{max}(1,2\text{-DCE}) - (1.32\pm0.23)\ 10^{-31}\ n_{DMA} -$$

$$- (2.33\pm0.84)\ 10^{-31}\ n_{CN}/n_{DMA}, \qquad (5)$$

$$n = 12,\ s = 2.67\ 10^{-31},\ R = 0.954.$$

The first-order polarizability α increases with increasing λ_{max} in 1,2-dichloroethane (1,2-DCE, polarizable solvent, this also holds true for other similar solvents) and, on the contrary, with the decreasing number of DMA units and the ratio of CN to DMA units. The negative sign of the wavenumber $\tilde{\nu}_{max}$(1,2-DCE) implies that more polarizable molecules have the longest-wavelength absorption maxima shifted bathochromically. The signs of the structural characteristics in equation (5) are somewhat surprising. The reason is probably an "electron rigidity" as a result of the D-π-A molecule polarization. Equation (5) can be used to evaluate the polarizability of organic D-π-A molecules in general.

CONCLUSION

A representative data set of the electronic absorption spectra of twelve systematically selected organic D-π-A molecules as solvatochromic indicators measured in 32 solvents allowed the application of a multidimensional statistic analysis and interpretation of the structure-property relationships. Simple structural characteristics based on a number or presence of specific structural features of the molecule showed to be suitable parameters in the correlation analysis. The most important characteristics are the number of DMA and CN groups, their ratio, and eventually the number of triple bond π-linkers. The quantum-chemically calculated molecule parameters such as LUMO energy, permanent dipole moment, COSMO area, and COSMO volume proved to be suitable structural characteristics as well. Whereas the solvent polarizability [$(n^2-1)/(n^2+2)$ function] and the solvent cavity size (molar volume V_m and Hildebrand δ_H) are the main factors affecting the position of λ_{max}, the solvent polarity (the Born function $1/\varepsilon_r$) is less important. The correlation dependencies are statistically valid and relatively strong. A relation between the first-order polarizability α, the longest-wavelegth absorption maxima λ_{max}, and the structural features has also been found. The higher-order polarizabilities β and γ are not related to the observed solavtochromism of indicators **1**–**12**.

EXPERIMENTAL SECTION

The complete synthesis and full spectral characterization of compounds **1**–**12** has been reported previously.[12-18] Solvents used for the solvatochromism study were chosen according to their specific difference (acidity, basicity, polarity, polarizability, and their combinations).[21] Solvents were reagent-grade and were purified by methods described in the literature.[10] The measured solution of compounds **1-9** had a concentration of 6×10^{-5} mol/L. Absorbance was in the range from 0.1 to 1.0. If the compound was not completely dissolved, a filtered saturated solution was measured instead. In order to verify the concentration independency of the absorption maxima position and that the Lambert–Beer law was fully obeyed, spectra of indicators **1**–**9** at different concentrations ranging from 6.45×10^{-5} to 6.45×10^{-6} M were measured (as shown in SI). Electron absorption spectra were recorded on a Hewlett-Packard 8453 spectrophotometer in the range of wavelengths from 200 to 1100 nm with an accuracy of 0.5 nm. The longest-wavelength absorption maxima were numerically determined from the obtained smoothed dependencies of absorbance on wavelength.

Initial geometries of the compounds **1-12** were calculated by PM3 method (ArgusLab, Ref.[22]) and subsequently optimized by the PM6 method (MOPAC2009, Ref.[23]). Employing MOPAC2009, the following characteristics were further calculated: E_{HOMO} and E_{LUMO} energies, dipole moment, COSMO area, COSMO volume, molecular dimensions (MD) 1, 2, and 3, isotropic polarizability α, and average second- and third-order polarizabilities β and γ. The predicted electronic absorption spectra were calculated by the ZINDO-CI method (10 highest occupied MOs, 10 lowest unoccupied MOs, self consistent reaction field methanol) using the molecular geometry optimized by ArgusLab.[22] Experimental data were examined by exploratory analysis and subsequently treated by principal component analysis PCA, factor analysis FA, and multiple linear regressions MLR. The Program OPstat[24] was employed for all statistical calculations.

Acknowledgements

This work was supported by the Ministry of Education, Youth and Sport of the Czech Republic (MSM 0021627501) and by the ETH Research Council.

REFERENCES

1. Special issue on "Organic Electronic and Optoelectronics", Eds. S. R. Forrest, M. E. Thompson, *Chem. Rev.* **2007**, *107*, 923–1386.
2. Special issue on "Materials for Electronics", Eds. R. D. Miller, E. A. Chandross, *Chem. Rev.* **2010**, *110*, 1–574.
3. G. S. He, L.-S. Tan, Q. Zheng, P. N. Prasad, *Chem. Rev.* **2008**, *108*, 1245.
4. M. Kivala, F. Diederich, *Acc. Chem. Res.* **2009**, *42*, 235.
5. M. Blanchard-Desce, V. Alain, P. V. Bedworth, S. R. Marder, A. Fort, C. Runser, M. Barzoukas, S. Lebus, R. Wortmann, *Chem. Eur. J.* **1997**, *3*, 1091.
6. (a) M. G. Kuzyk, *J. Mater. Chem.* **2009**, *19*, 7444; (b) J. C. May, I. Biaggio, F. Bureš, F. Diederich, *Appl. Phys. Lett.* **2007**, *90*, 251106.
7. F. Bureš, W. B. Schweizer, J. C. May, C. Boudon, J.-P. Gisselbrecht, M. Gross, I. Biaggio, F. Diederich, *Chem. Eur. J.* **2007**, *13*, 5378.
8. E. L. Spitler, L. D. Shirtcliff, M. M. Haley, *J. Org. Chem.* **2007**, *72*, 86.
9. J. Kulhánek, F. Bureš, O. Pytela, T. Mikysek, J. Ludvík, A. Růžička, *Dyes Pigm.* **2010**, *85*, 57.
10. F. Bureš, O. Pytela, F. Diederich, *J. Phys. Org. Chem.* **2009**, *22*, 155.
11. F. Bureš, W. B. Schweizer, C. Boudon, J.-P. Gisselbrecht, M. Gross, F. Diederich, *Eur. J. Org. Chem.* **2008**, 994.
12. N. N. P. Moonen, C. Boudon, J.-P. Gisselbrecht, P. Seiler, M. Gross, F. Diederich, *Angew. Chemie.* **2002**, *114,* 3170; *Angew. Chem. Int. Ed.* **2002**, *41*, 3044.
13. N. N. P. Moonen, R. Gist, C. Boudon, J.-P. Gisselbrecht, P. Seiler, T. Kawai, A. Kishioka, M. Gross, M. Irie, F. Diederich, *Org. Biomol. Chem.* **2003**, *1*, 2032.
14. N. N. P. Moonen, W. C. Pomerantz, R. Gist, C. Boudon, J.-P. Gisselbrecht, T. Kawai, A. Kishioka, M. Gross, M. Irie, F. Diederich, *Chem. Eur. J.* **2005**, *11*, 3325.
15. M. Kivala, C. Boudon, J.-P. Gisselbrecht, P. Seiler, M. Gross, F. Diederich, *Chem. Commun.* **2007**, 4731.
16. T. Michinobu, J. C. May, J. H. Lim, C. Boudon, J.-P. Gisselbrecht, P. Seiler, M. Gross, I. Biaggio, F. Diederich, *Chem. Commun.* **2005**, 737.
17. T. Michinobu, C. Boudon, J.-P. Gisselbrecht, P. Seiler, B. Frank, N. N. P. Moonen, M. Gross, F. Diederich, *Chem. Eur. J.* **2006**, *12*, 1889.
18. M. Kivala, T. Stanoeva, T. Michinobu, B. Frank, G. Gescheidt, F. Diederich, *Chem. Eur. J.* **2008**, *14*, 7638.

19. S. Wold, P. Geladi, K. Esbensen, J. Ohman, *J. Chemometrics* **1978**, *1*, 41.
20. O. Exner, *Collect. Czech. Chem. Commun.* **1976**, *41*, 1516.
21. (a) O. Pytela, *Collect. Czech. Chem. Commun.* **1990**, *55*, 644; (b) A. J. Parker, *Quart. Rev. (London)* **1962**, *16*, 163.
22. ArgusLab, Mark Thompson and Planaria Software LLC, Version 4.01,webpage: http://www.arguslab.com
23. MOPAC2007, J. J. P. Stewart, Stewart Computational Chemistry,version 8.315W, webpage: http://OpenMOPAC.net.
24. OPstat, O. Pytela, version 6.25, webpage: http://webak.upce.cz/~koch/cz/veda/OPgm.htm.
25. C. Reichardt, *Solvents and Solvent Effects in Organic Chemistry*, Wiley-VCH, Weinheim, **2004**.

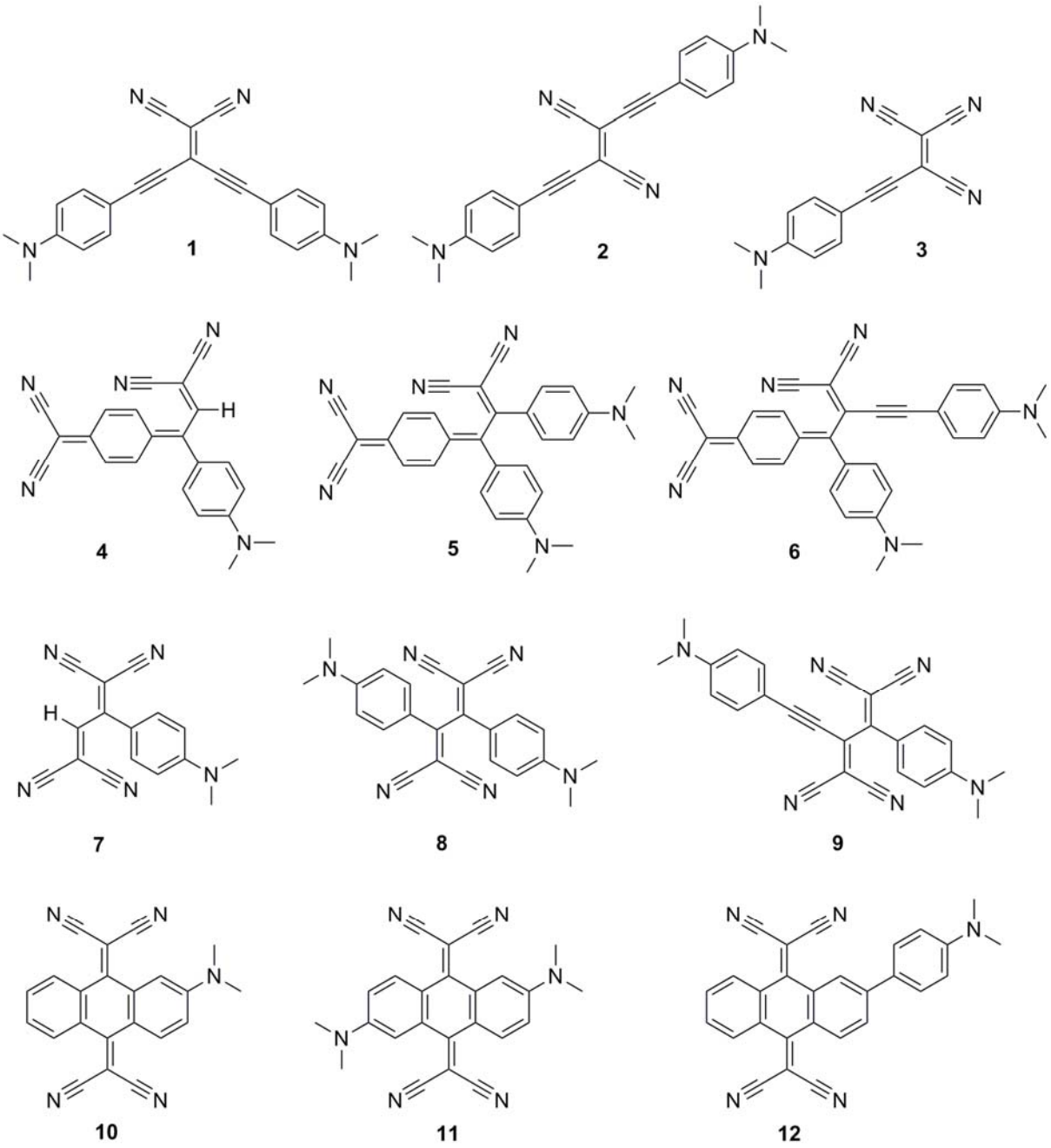

Figure 1. Molecular structures of compounds **1-12**: CEEs (**1-3**), TCNQ-based (**4-6**), TCBDs (**7-9**), and TCAQs (**10-12**).

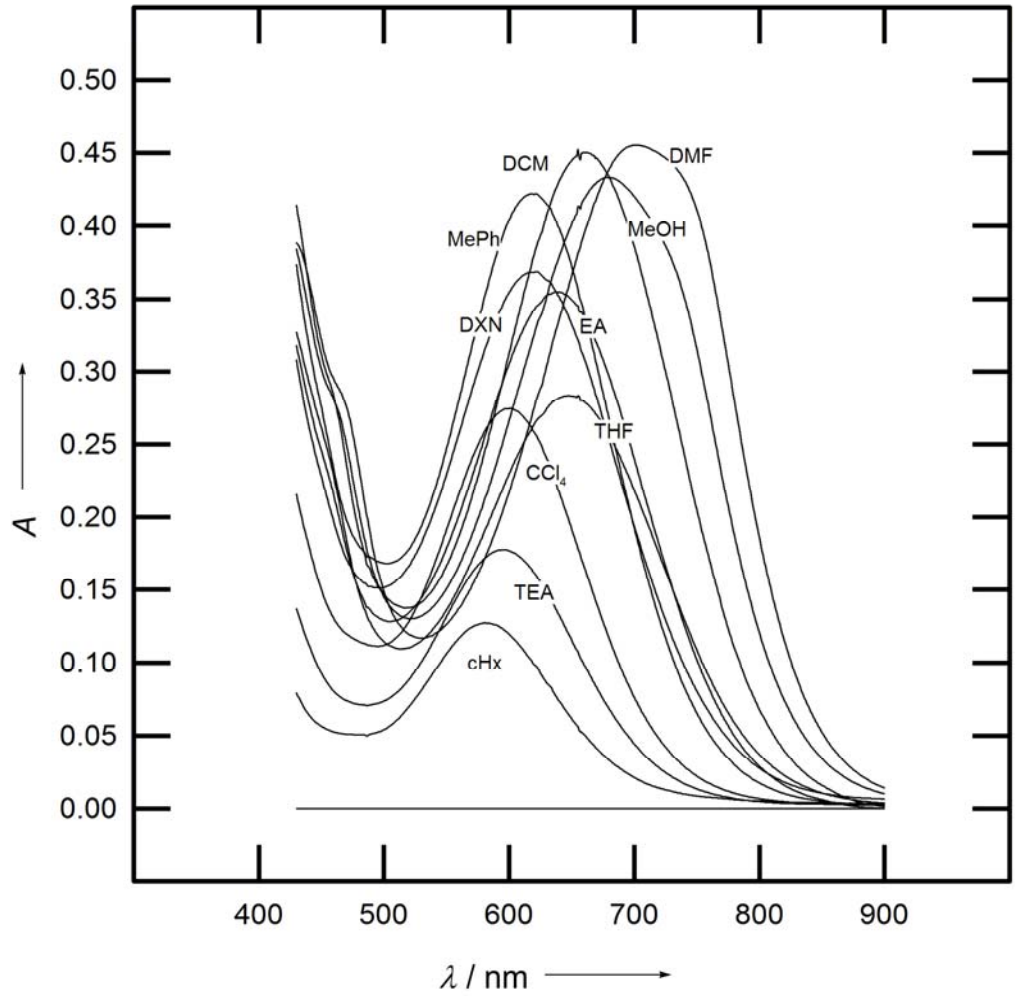

Figure 2. UV/Vis spectra of the organic charge-transfer compound **5**, measured in the selected solvents (cHx – cyclohexane, TEA – triethylamine, CCl_4 – tetrachloromethane, MePh – toluene, DXN – 1,4-dioxane, THF – tetrahydrofuran, EA – ethyl acetate, DCM – dichloromethane, DMF – *N*,*N*-dimethylformamide, MeOH – methanol).

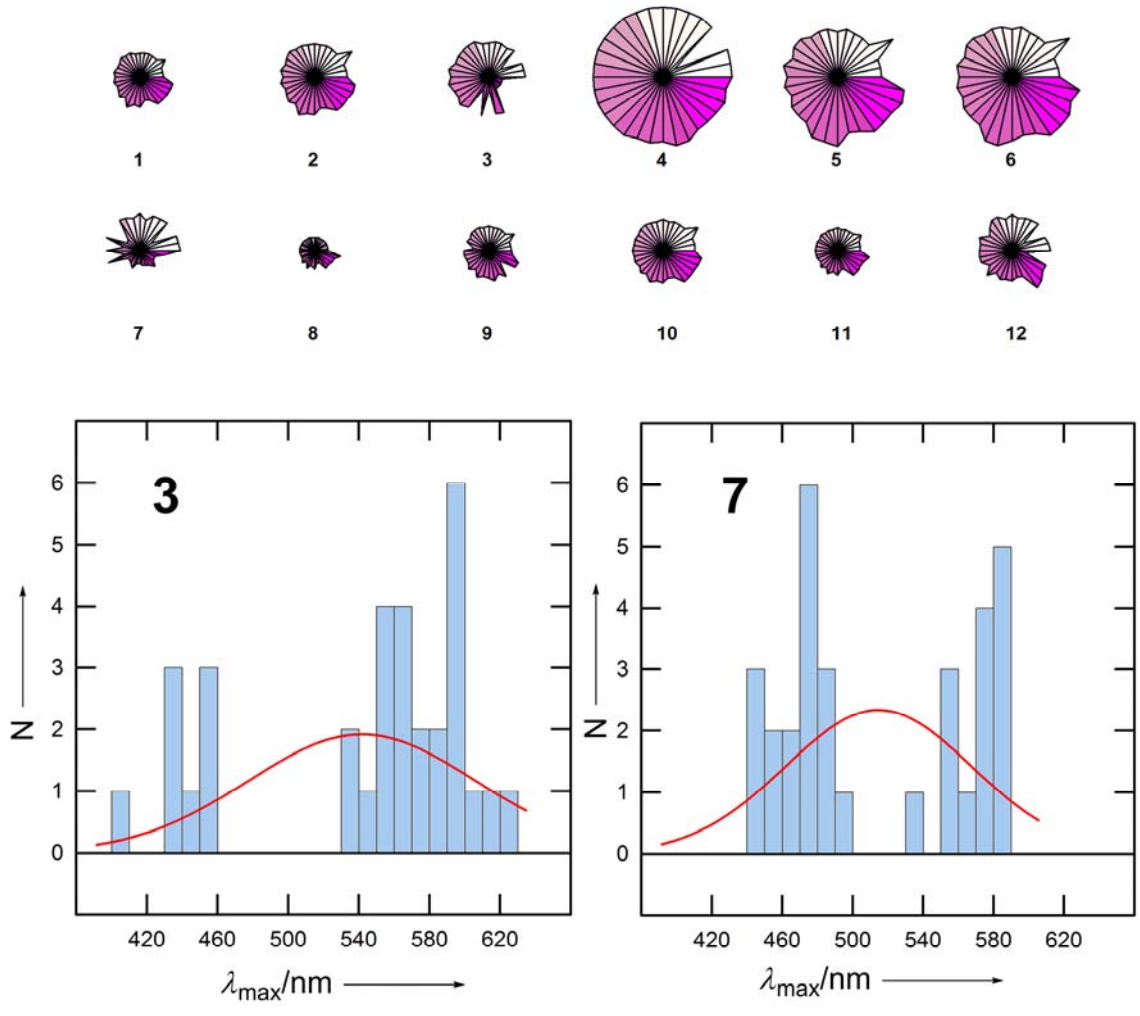

Figure 3. The mutual relationships of λ_{max} for compounds **1–12**, depicted as polygons (the polygon's rays correspond to the 32 solvents), the λ_{max} histograms for indicators **3** and **7**, and the frequency function of normal distribution, N.

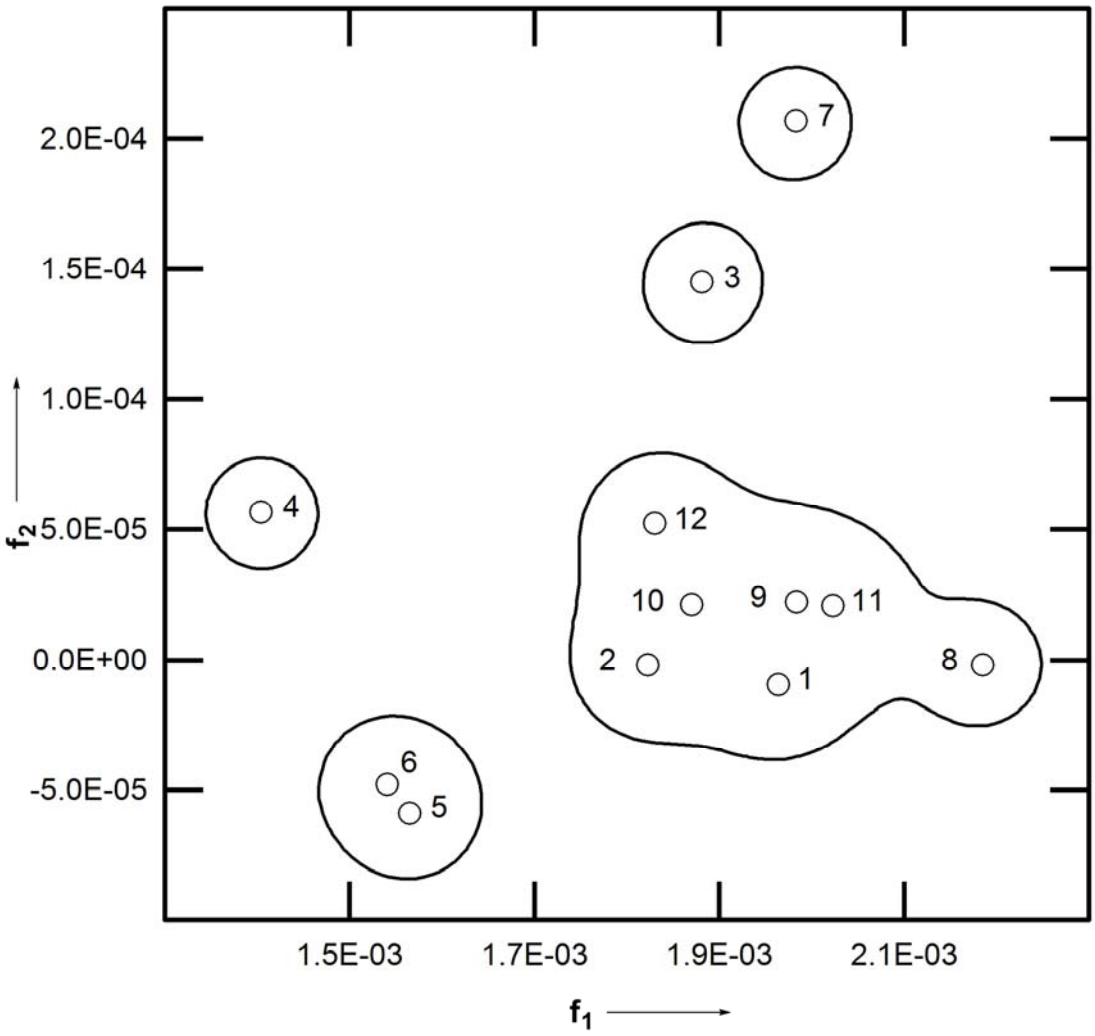

Figure 4. Relationships of points corresponding to compounds **1-12** in the plane of the first two factors; the clusters were created by implicit function.

Table 1. The longest-wavelength absorption maxima λ_{max} of the intramolecular CT bands measured for compounds **1-9** in dependence on 32 solvents (listed in ascending order according to solvent's E_T^N values[25]).

Solvent	Wavelength λ_{max} [nm]								
	1	**2**	**3**	**4**	**5**	**6**	**7**	**8**	**9**
Cyclohexane	489	529	544	695	581.5	594	561.5	440	483
n-Hexane	482	521	535	687	570	588	553	438	478
n-Heptane	484	522.5	537	693	576.5	585	554	438	479
Triethylamine	492.5	533	445.5	- [a]	594.5	604	- [a]	445	492
Tetrachloromethane	498.5	539	555	722.5	600	611	572.5	448.5	496
Toluene	510	554	563.5	738.5	618.5	629.5	582	462	514
Benzene	513	557	567.5	742.5	623	632.5	585	464	518
Diethyl ether	500	541	555.5	716.5	615	626.5	534	454	500
m-Xylene	506.5	551	559.5	735.5	615.5	626	576.5	461	512.5
1,4-Dioxane	499.5	545.5	551	719.5	618.5	628.5	550.5	459	507.5
Bromobenzene	532.5	572	596.5	770.5	656	668	588	472.5	531
Chlorobenzene	526.5	568	591.5	766	650.5	663	588	470	527.5
Tetrahydrofuran	519	560.5	567	737	648	661.5	471	456.5	512.5
Ethyl acetate	511.5	550	564	721.5	638	650	467	464	506
Chloroform	522	562	590.5	775	654	668.5	589	468	524
Pyridine	539	580	618	766.5	688.5	692	483.5	478	- [a]
Dichloromethane	524.5	563	593	765	660.5	675	571	470	525.5
Nitrobenzene	547.5	585	624	781.5	695	706	485	481	539
1,2-Dichloroethane	524	564	594	767	661.5	676	572	471	525.5
Butan-2-one	526	563	578	738.5	668.5	679	473	470	516.5
Benzonitrile	539.5	579	605	771.5	689.5	704	460	478.5	536
Acetone	522	561	576.5	735	670.5	681	474	471	515.5
N,*N*-Dimethylacetamide	539.5	579	451.5	702.5	699.5	716	476	480	525.5
N,*N*-Dimethylformamide	536.5	577.5	587	708.5	703.5	718.5	472	479	526
Dimethyl sulfoxide	545.5	586	459.5	721	745.5	719	459.5	485	531
Acetonitrile	520.5	560	583	732	676	686.5	480	473	550
Nitromethane	528	566.5	593.5	731	688	697	484.5	476	528
Propan-2-ol	515.5	554.5	432	654.5	671	683	447	467	507.5
Benzyl alcohol	545.5	585	452	697.5	707	727	491	483.5	457
Ethanol	524	559.5	433.5	675	678.5	701	450	469	516.5
Methanol	520	557	434	669.5	679.5	652.5	443	470	514
Formamide	531	580	401.5	723.5	747	753.5	464.5	486.5	550
$\Delta\lambda_{max}$/nm (Formamide-cHx)[b]	42	51	-142.5	28.5	165.5	159.5	-97	46.5	67

[a] Not measurable.

[b] Indicators **1**, **2**, **4**, **5**, **6**, **8**, and **9** are positively solvatochromic; indicators **3** and **7** are negatively solvatochromic.

Table 2. The factor loadings $\mathbf{f}_1$ and $\mathbf{f}_2$, calculated for compounds **1-12** by nonlinear regression using the two-factor model.

Indicator	**1**	**2**	**3**	**4**	**5**	**6**	**7**	**8**	**9**	**10**	**11**	**12**
10^3 $\mathbf{f}_1$	1.964	1.823	1.881	1.404	1.565	1.541	1.983	2.185	1.984	1.870	2.023	1.831
10^6 $\mathbf{f}_2$	-9.573	-1.991	144.9	56.47	-58.97	-47.96	206.7	-1.867	21.97	20.99	20.69	52.22

Table 3. The characteristics of compounds **1-12**, calculated by the PM6 method (MOPAC2009).

Indicator	COSMO area [Å^2]	COSMO volume [Å^3]	E_{HOMO} [eV]	E_{LUMO} [eV]	MD1 [Å]	MD2 [Å]	MD3 [Å]	Dipole moment [D]	$10^{30}\,\alpha$ [esu]	$10^{29}\,\beta$ [esu]	$10^{27}\,\gamma$ [esu]
1	439.39	468.57	-8.36	-1.42	18.6	8.9	1.9	11.2	3.43	2.99	4.61
2	438.61	468.93	-8.11	-1.45	21.1	6.0	1.7	2.4	3.70	0.27	8.25
3	303.06	312.56	-8.66	-2.03	13.5	6.1	1.6	11.3	2.17	5.07	2.78
4	392.90	441.67	-8.76	-2.30	13.3	13.2	5.5	9.9	3.16	1.41	-0.47
5	497.18	591.40	-8.59	-2.16	13.8	13.3	7.8	12.4	4.23	2.38	1.09
6	540.82	623.56	-8.57	-2.13	14.6	13.0	8.2	13.1	4.70	4.45	2.96
7	314.06	347.39	-8.80	-1.96	10.7	7.9	4.9	8.3	2.06	2.63	1.13
8	418.21	498.43	-8.61	-1.69	14.9	7.7	6.6	8.0	3.16	3.01	2.37
9	460.68	531.87	-8.57	-1.70	16.5	8.7	7.6	11.1	3.57	4.09	3.50
10	363.09	421.49	-8.86	-2.19	11.0	7.7	5.6	8.1	2.72	1.82	1.13
11	406.67	480.57	-8.72	-1.98	13.5	7.9	4.2	7.2	3.15	1.73	1.89
12	442.15	515.94	-8.41	-2.24	15.3	8.3	6.4	8.4	3.40	3.20	2.58

Table of Contents

Solvatochromism as an efficient tool to study *N*,*N*-dimethylamino- and cyano-substituted π-conjugated molecules with an intramolecular charge-transfer absorption

Filip Bureš, Oldřich Pytela, Milan Kivala, and François Diederich

Electronic absorption spectra of twelve systematically chosen charge-transfer D-π-A push-pull systems featuring electron-withdrawing CN groups, electron-donating $N(CH_3)_2$ groups, and various π-conjugated backbones have been measured in 32 solvents. The solvent polarizability and the solvent cavity size proved to be the most crucial factors affecting the position of λ_{max}. The most important characteristics of D-π-A molecules concerning the solvatochromism are the energy of LUMO, the permanent dipole moment, the COSMO area, the COSMO volume, the number of donors/acceptors, and the length of the π-conjugated path.

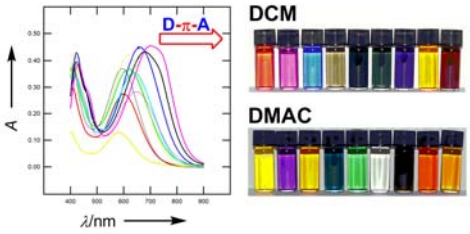

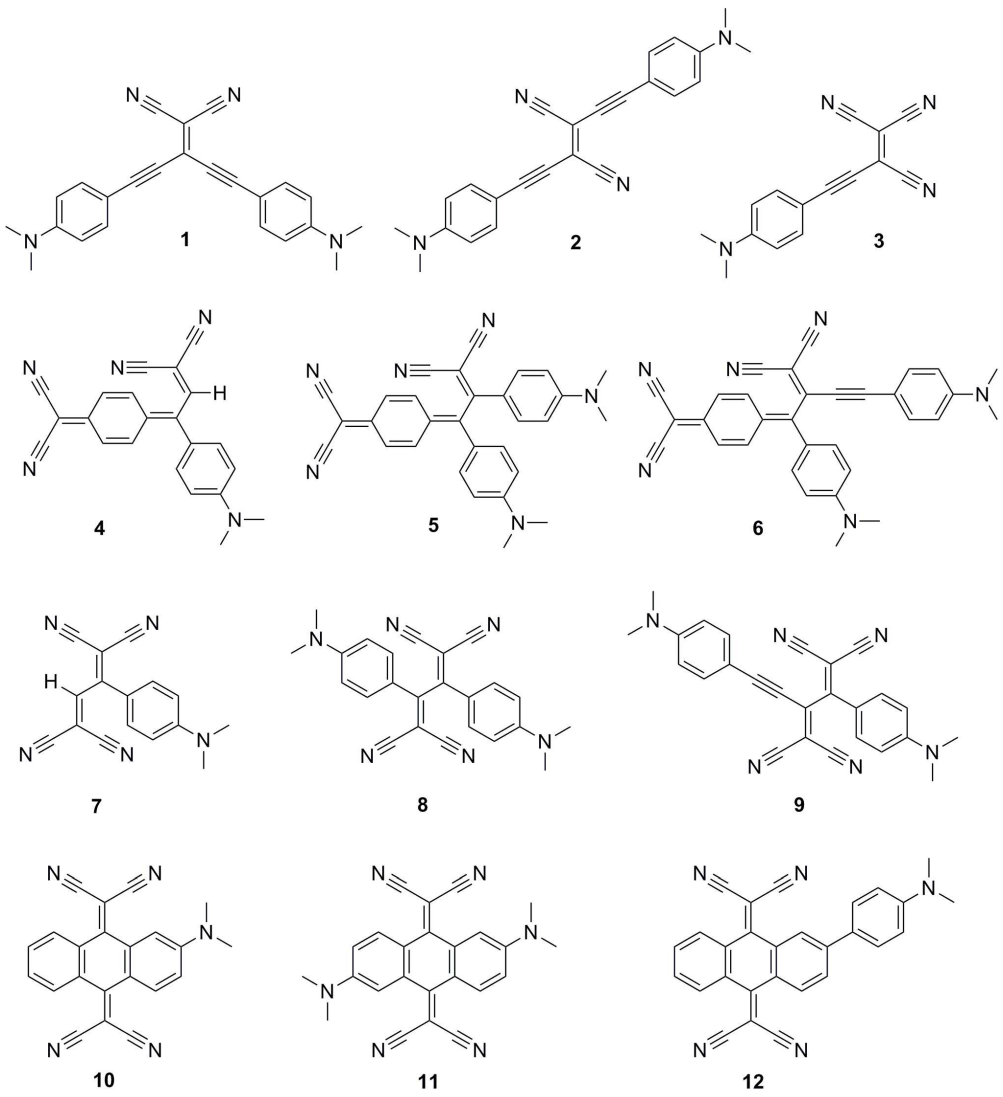

172x188mm (300 x 300 DPI)

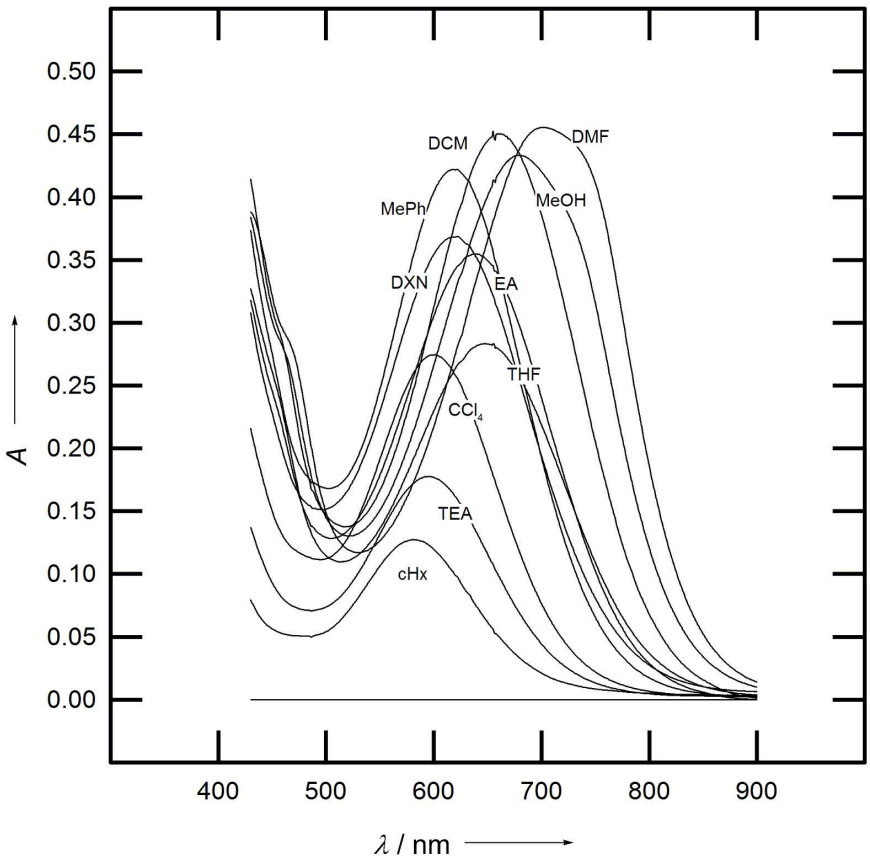

153x153mm (600 x 600 DPI)

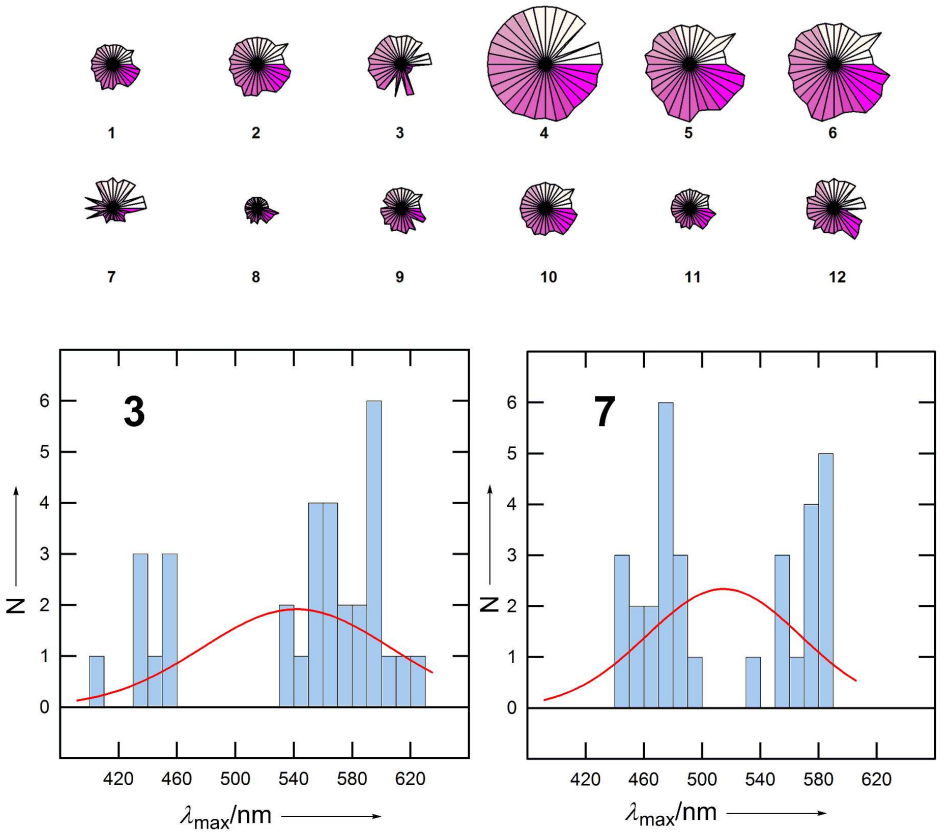

166x158mm (600 x 600 DPI)

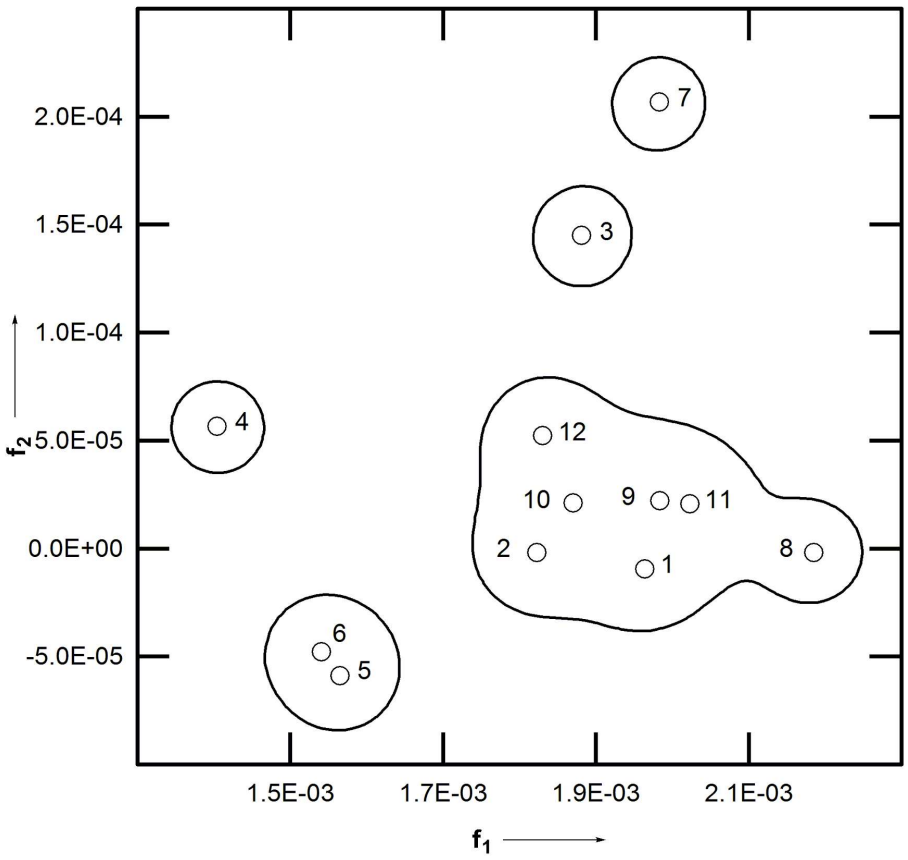

162x162mm (600 x 600 DPI)

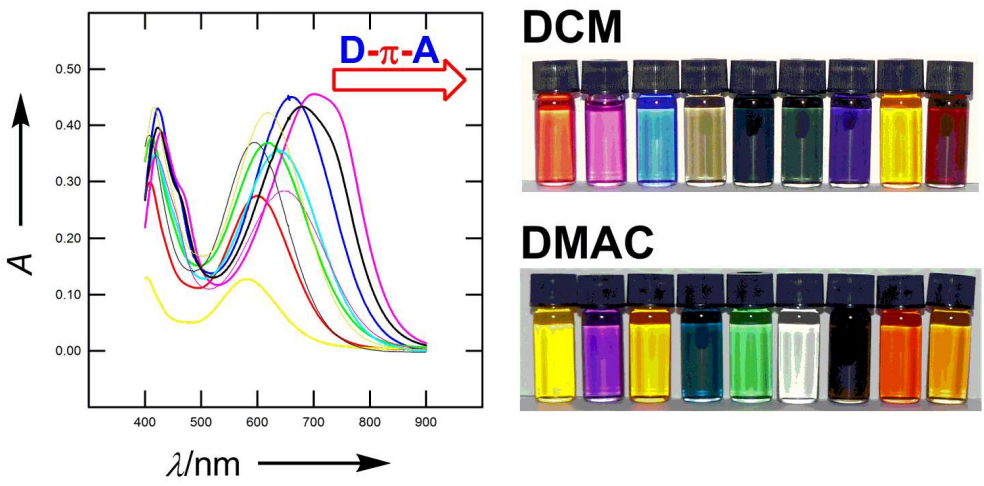

62x34mm (600 x 600 DPI)

Supporting information for

J. Phys. Org. Chem.

Solvatochromism as an efficient tool to study *N*,*N*-dimethylamino- and cyano-substituted π-conjugated molecules with an intramolecular charge-transfer absorption

Filip Bureš, Oldřich Pytela, Milan Kivala and François Diederich

Table of Contents Page

UV/Vis spectra of compound 1.

The spectra are listed in ascending order according to E_T^N values (see Table 1, main text).

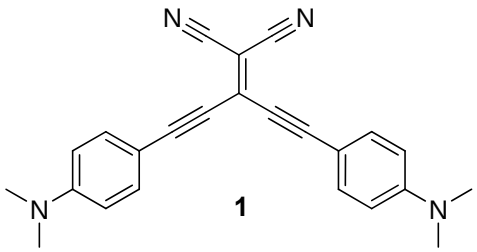

Figure 1SI. UV/VIS spectra of compound **1** in selected solvents (part 1).

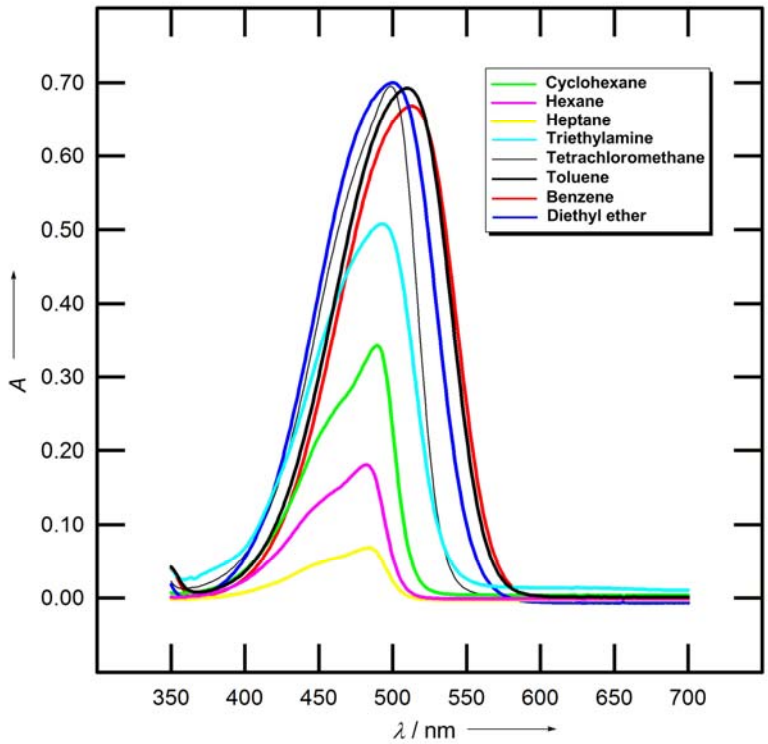

Figure 2SI. UV/VIS spectra of compound **1** in selected solvents (part 2).

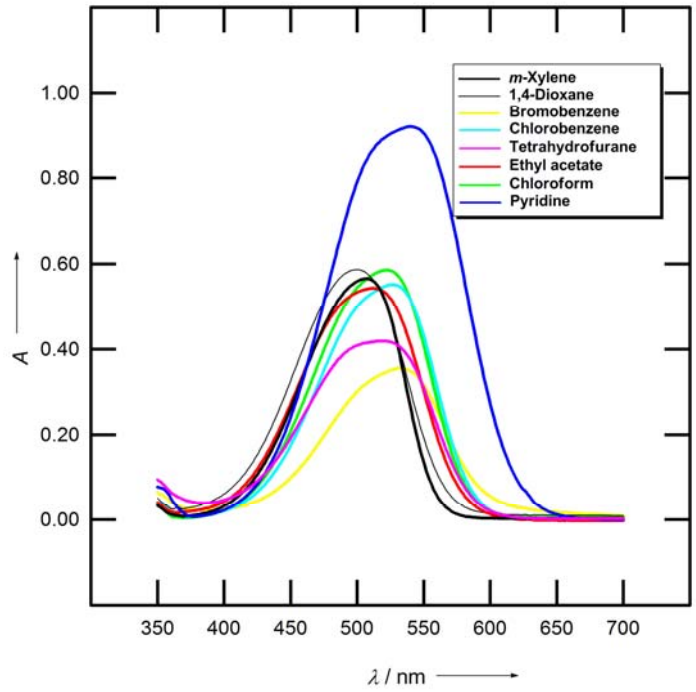

Figure 3SI. UV/VIS spectra of compound **1** in selected solvents (part 3).

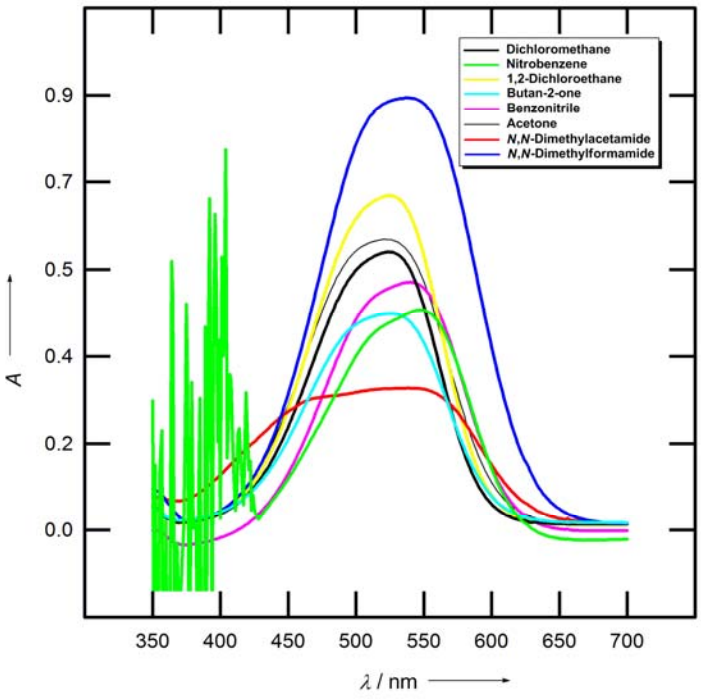

Figure 4SI. UV/VIS spectra of compound **1** in selected solvents (part 4).

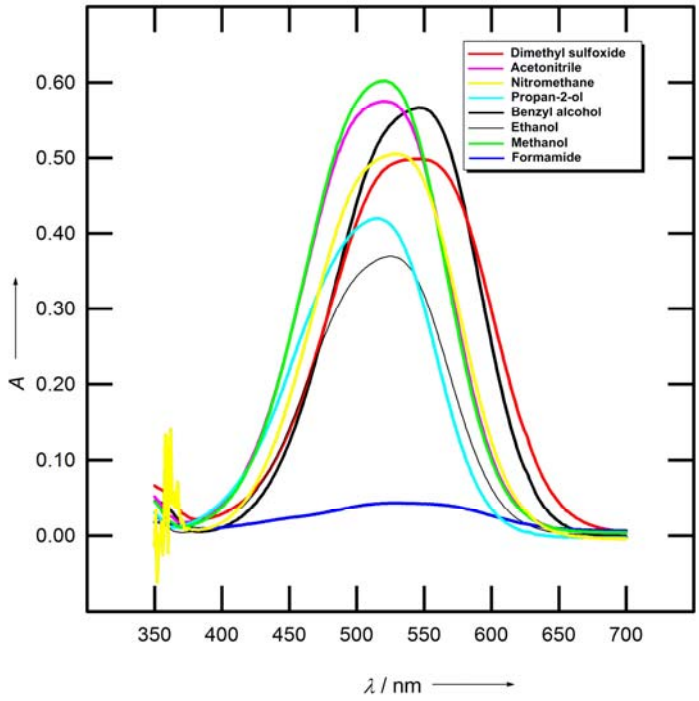

Figure 5SI. UV/VIS spectra of compound **1** in CH_2Cl_2 – dependence on concentration.

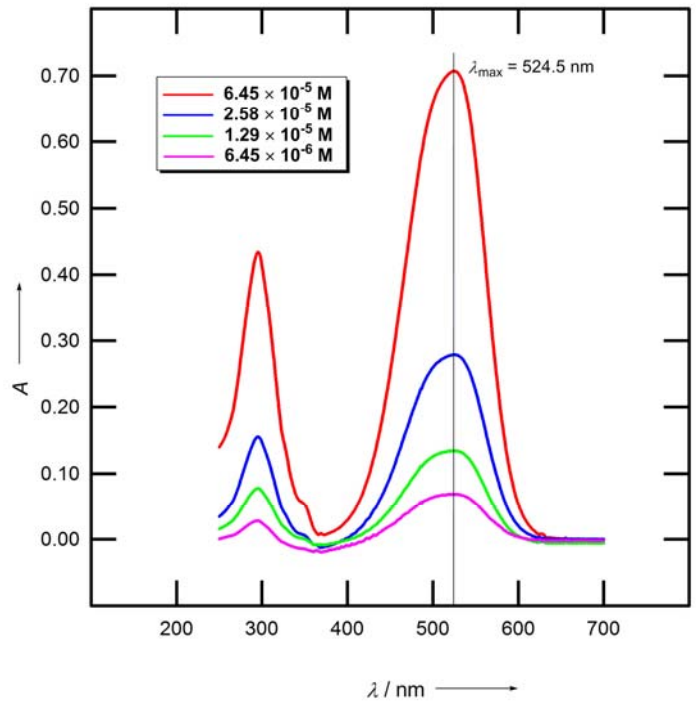

UV/Vis spectra of compound 2.

The spectra are listed in ascending order according to E_T^N values (see Table 1, main text).

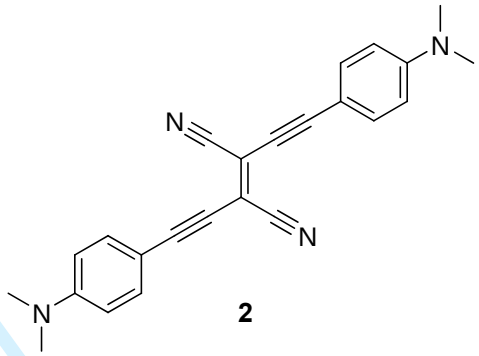

2

Figure 6SI. UV/VIS spectra of compound **2** in selected solvents (part 1).

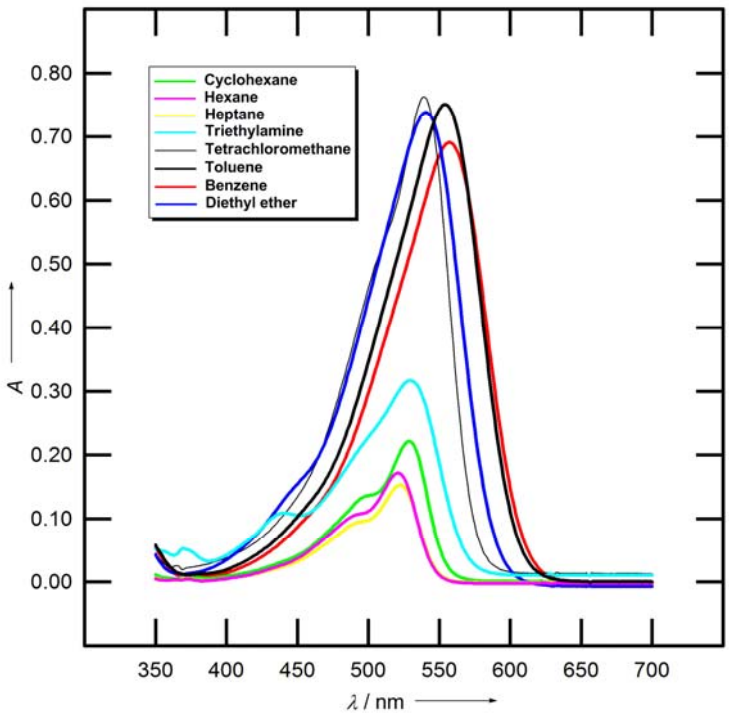

Figure 7SI. UV/VIS spectra of compound **2** in selected solvents (part 2).

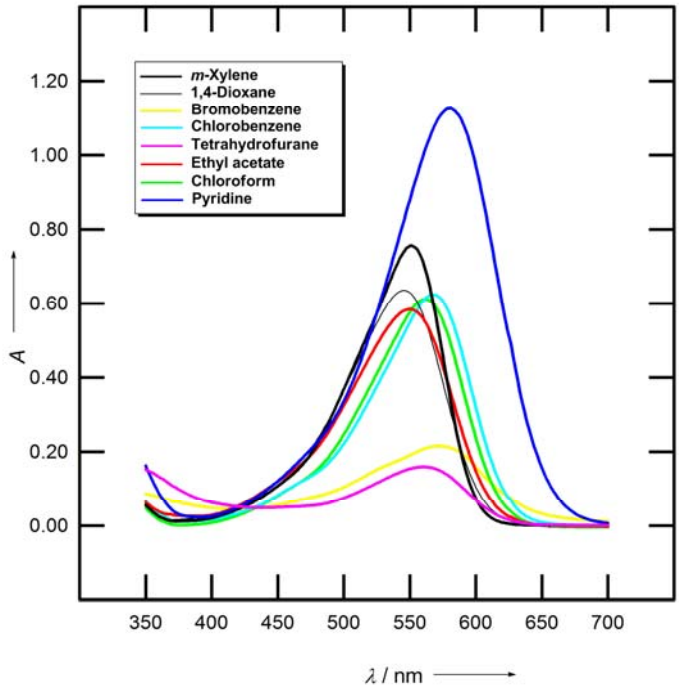

Figure 8SI. UV/VIS spectra of compound **2** in selected solvents (part 3).

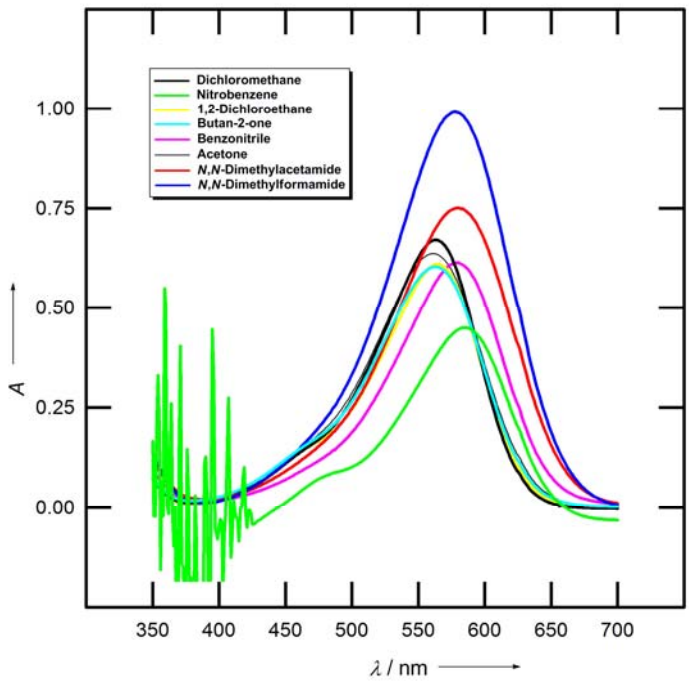

Figure 9SI. UV/VIS spectra of compound **2** in selected solvents (part 4).

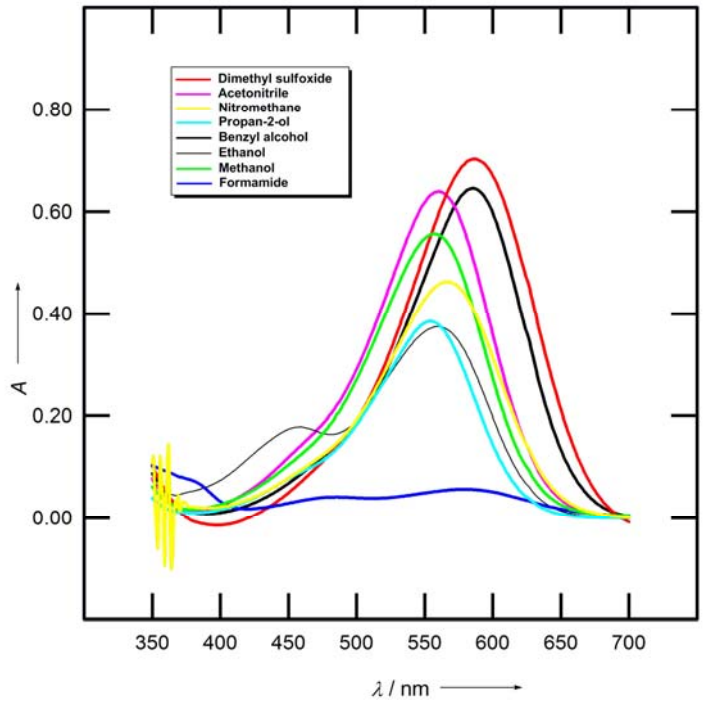

Figure 10SI. UV/VIS spectra of compound **2** in CH_2Cl_2 – dependence on concentration.

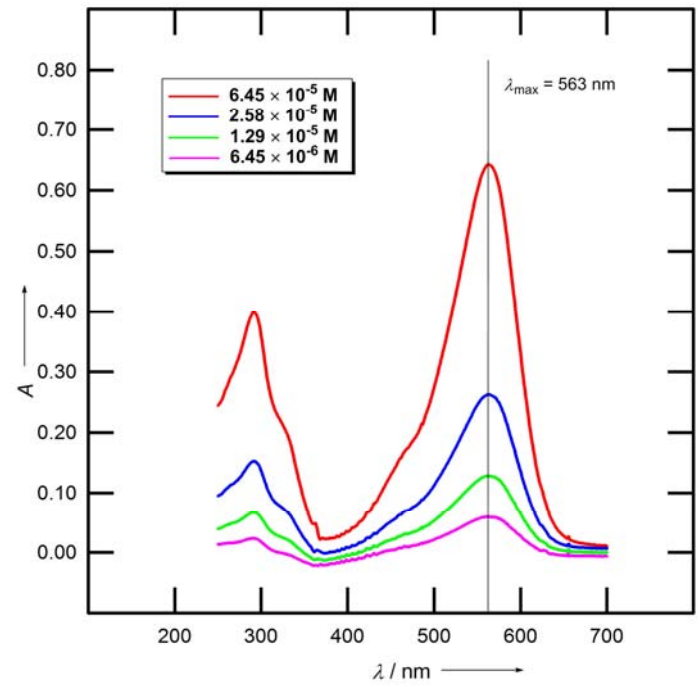

UV/Vis spectra of compound 3.

The spectra are listed in ascending order according to E_T^N values (see Table 1, main text).

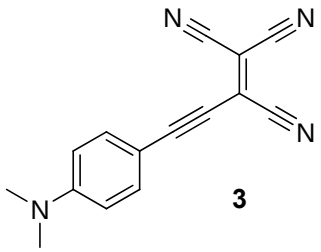

Figure 11SI. UV/VIS spectra of compound **3** in selected solvents (part 1).

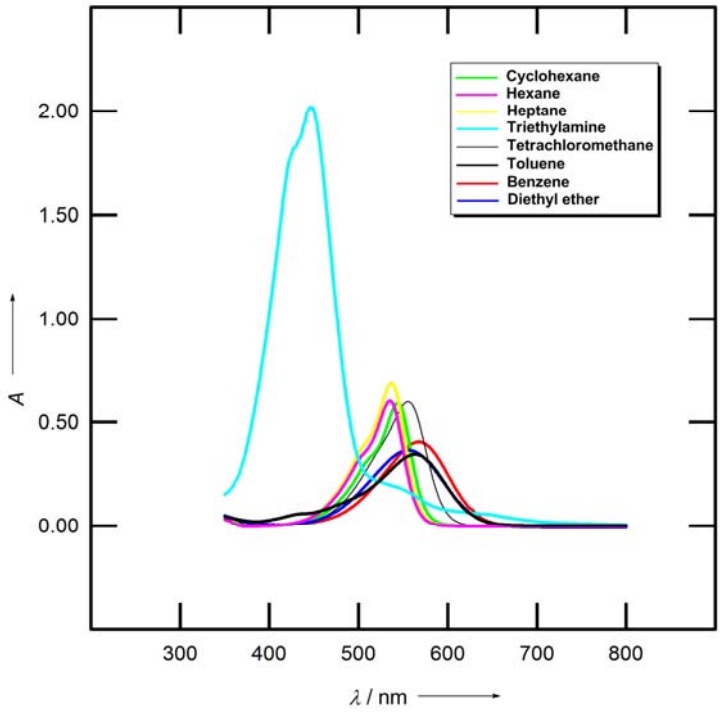

Figure 12SI. UV/VIS spectra of compound **3** in selected solvents (part 2).

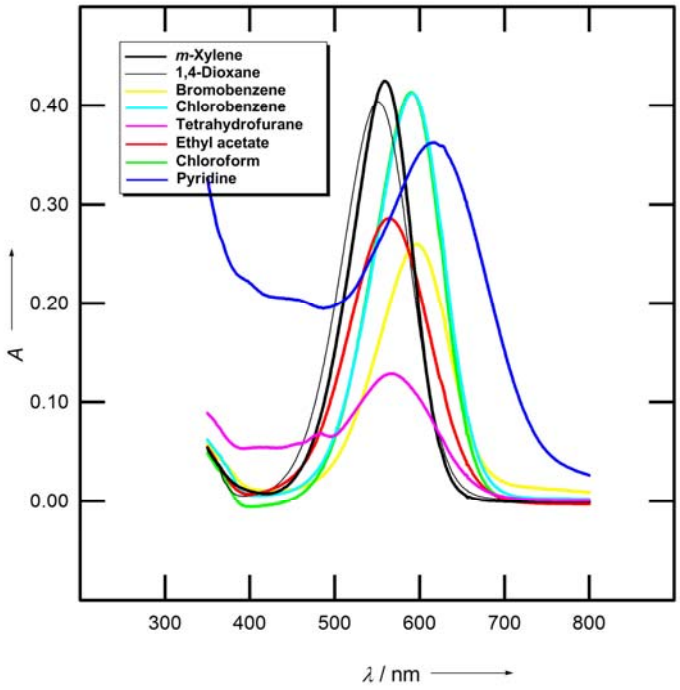

Figure 13SI. UV/VIS spectra of compound **3** in selected solvents (part 3).

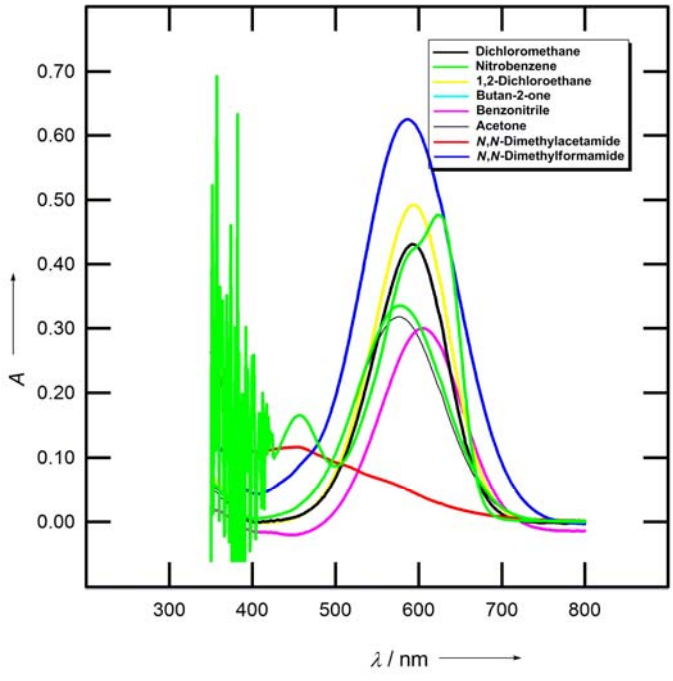

Figure 14SI. UV/VIS spectra of compound **3** in selected solvents (part 4).

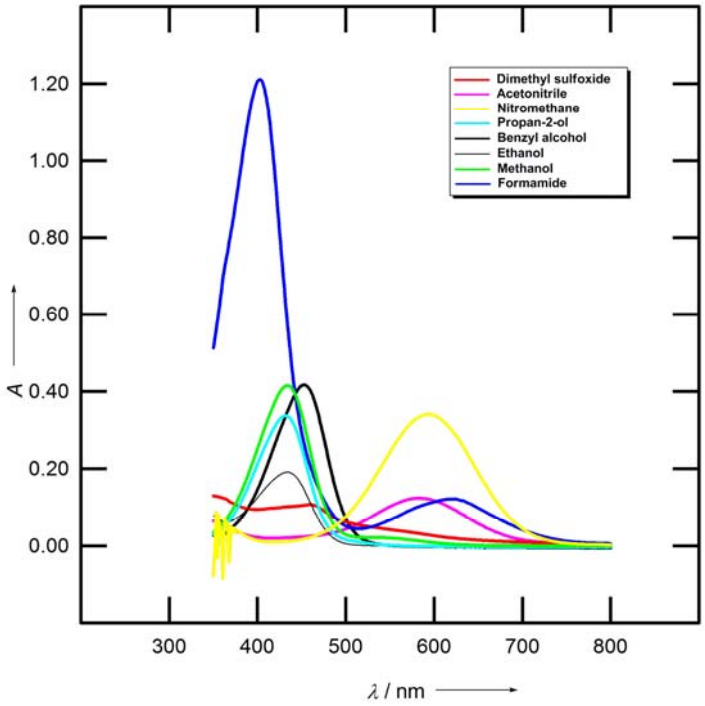

Figure 15SI. UV/VIS spectra of compound **3** in CH_2Cl_2 – dependence on concentration.

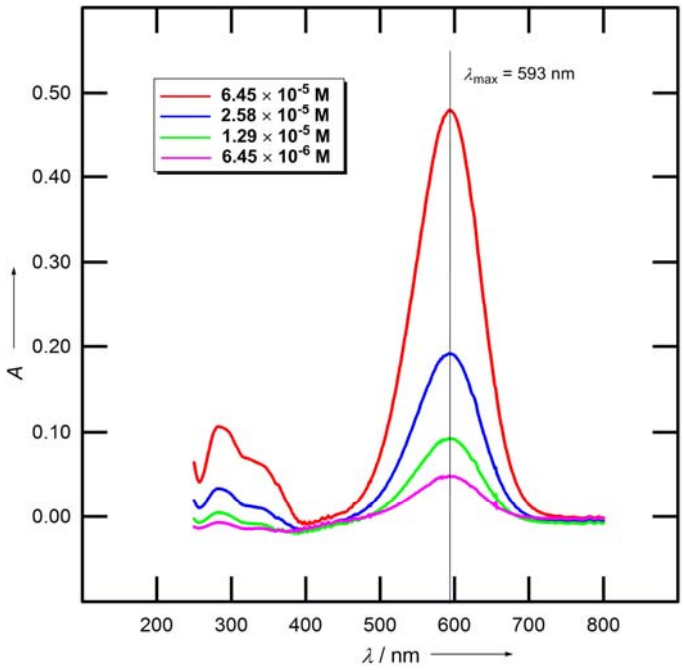

UV/Vis spectra of compound 4.

The spectra are listed in ascending order according to E_T^N values (see Table 1, main text).

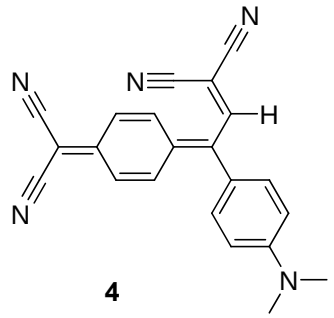

4

Figure 16SI. UV/VIS spectra of compound **4** in selected solvents (part 1).

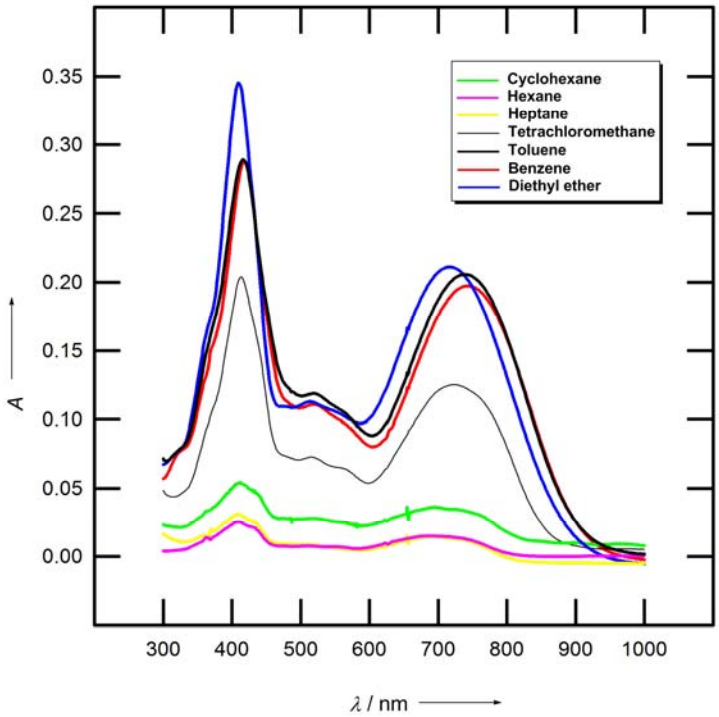

Figure 17SI. UV/VIS spectra of compound **4** in selected solvents (part 2).

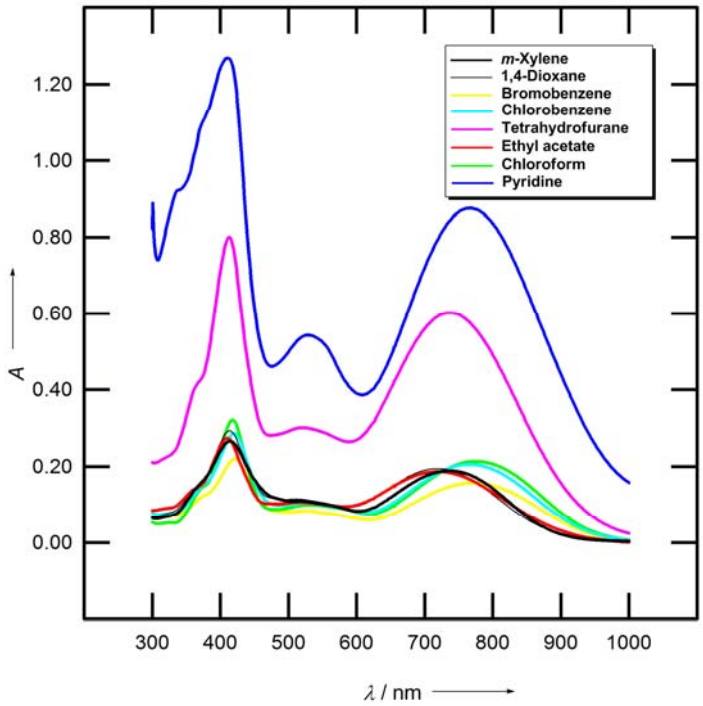

Figure 18SI. UV/VIS spectra of compound **4** in selected solvents (part 3).

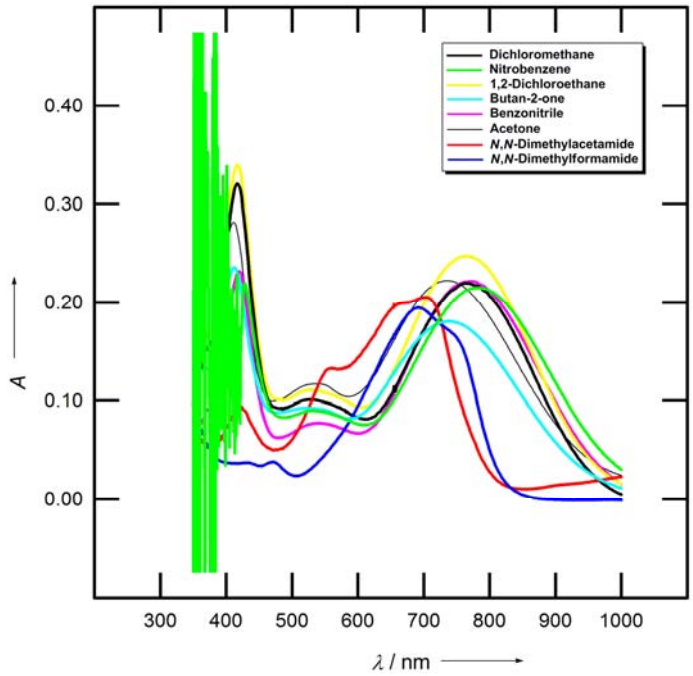

Figure 19SI. UV/VIS spectra of compound **4** in selected solvents (part 4).

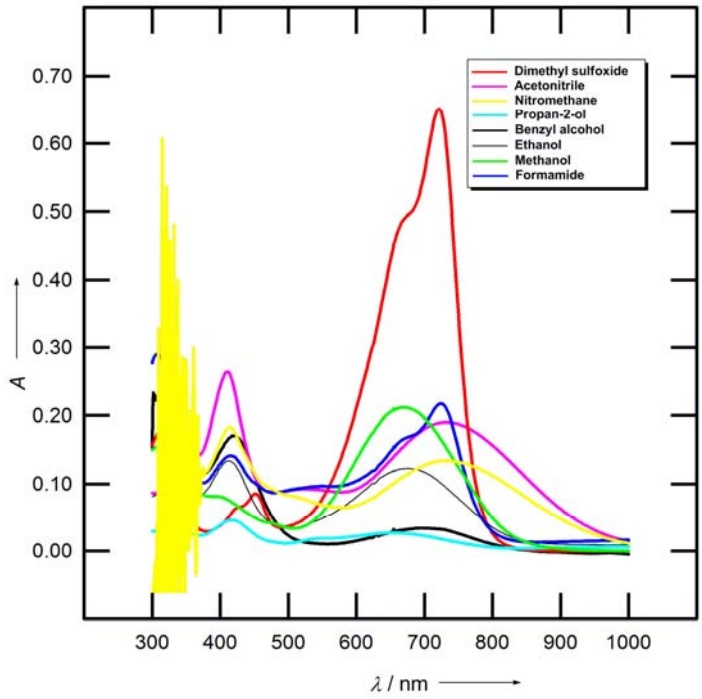

Figure 20SI. UV/VIS spectra of compound **4** in CH_2Cl_2 – dependence on concentration.

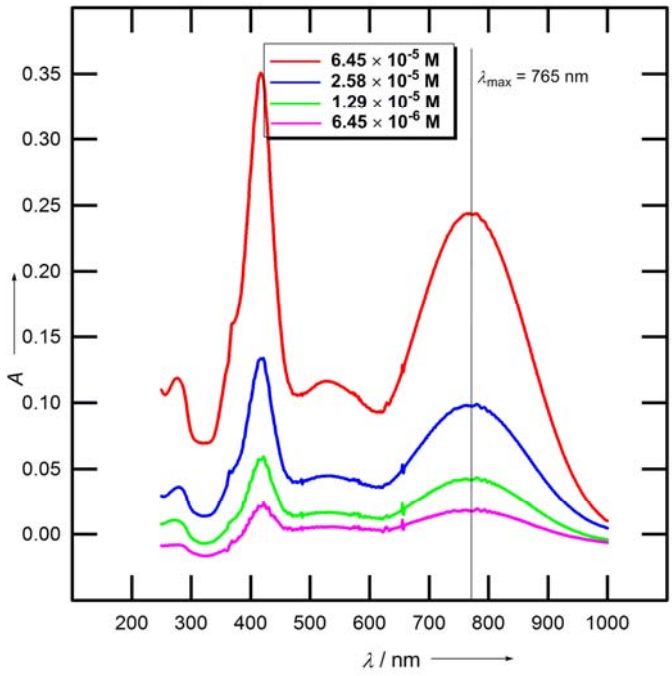

UV/Vis spectra of compound 5.

The spectra are listed in ascending order according to E_T^N values (see Table 1, main text).

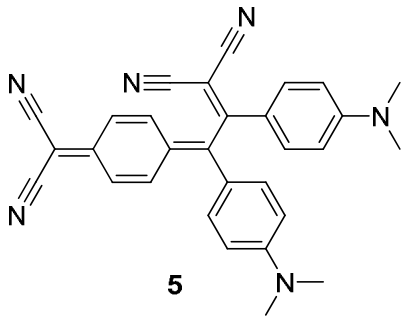

Figure 21SI. UV/VIS spectra of compound **5** in selected solvents (part 1).

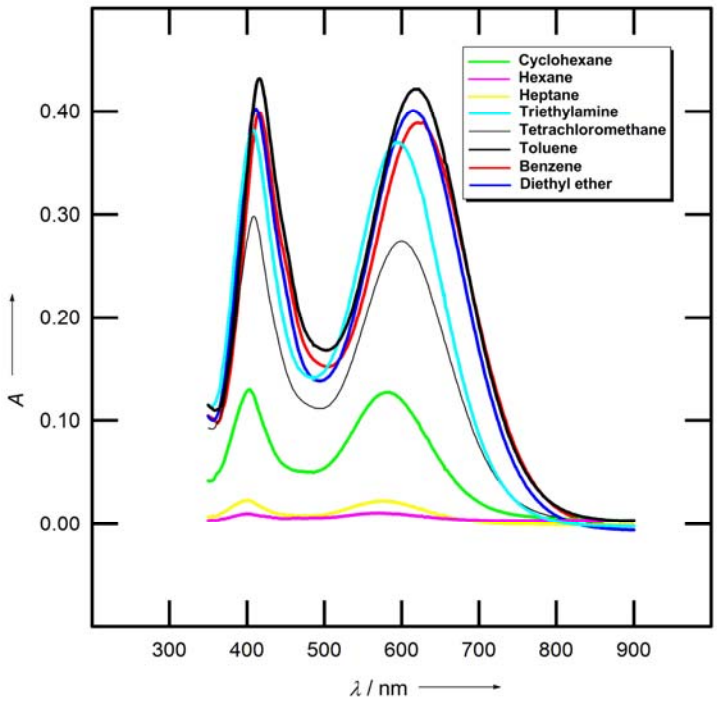

Figure 22SI. UV/VIS spectra of compound **5** in selected solvents (part 2).

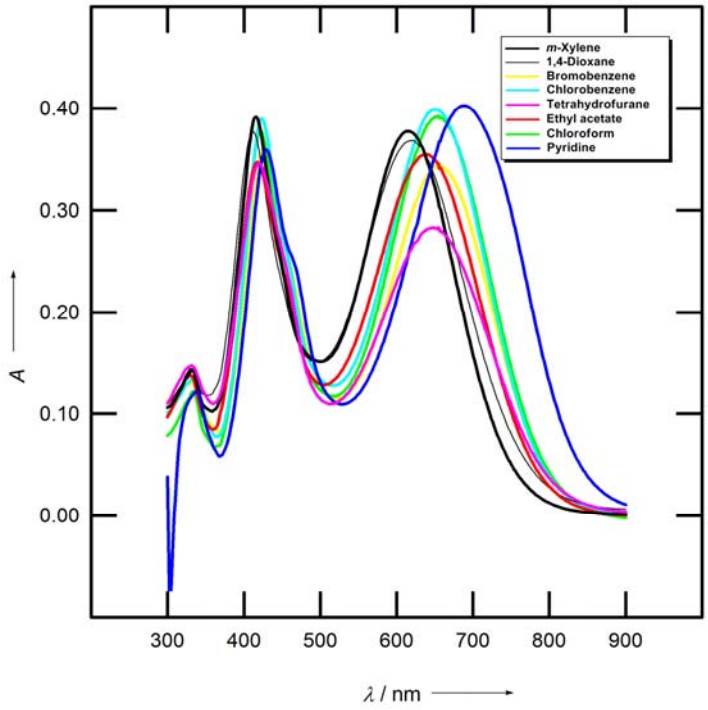

Figure 23SI. UV/VIS spectra of compound **5** in selected solvents (part 3).

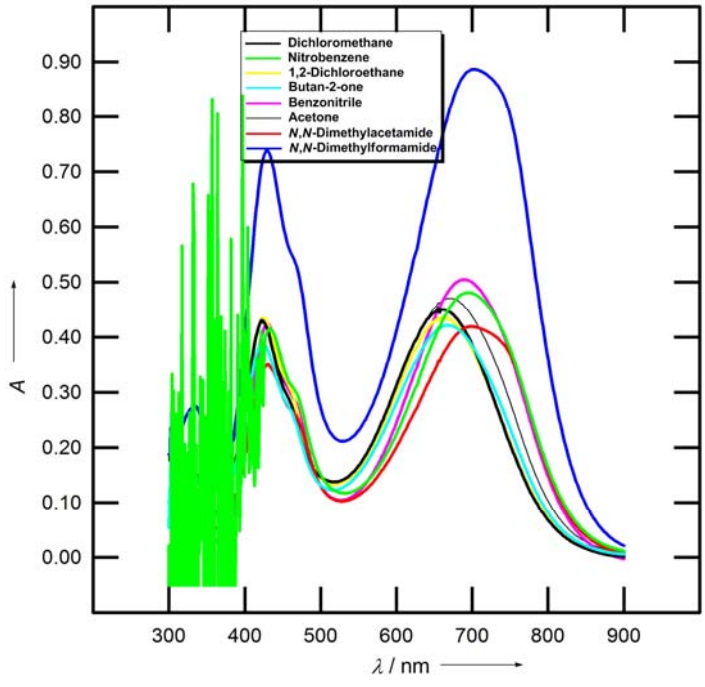

Figure 24SI. UV/VIS spectra of compound **5** in selected solvents (part 4).

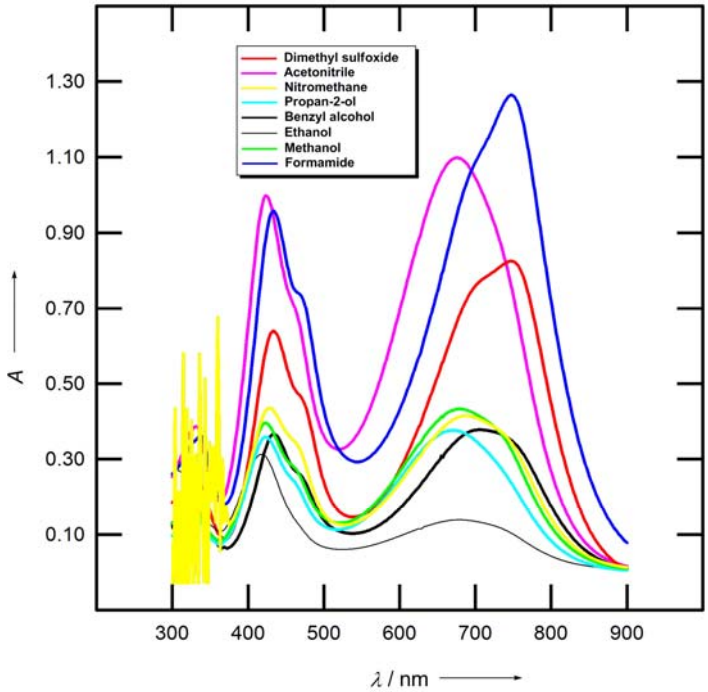

Figure 25SI. UV/VIS spectra of compound **5** in CH_2Cl_2 – dependence on concentration.

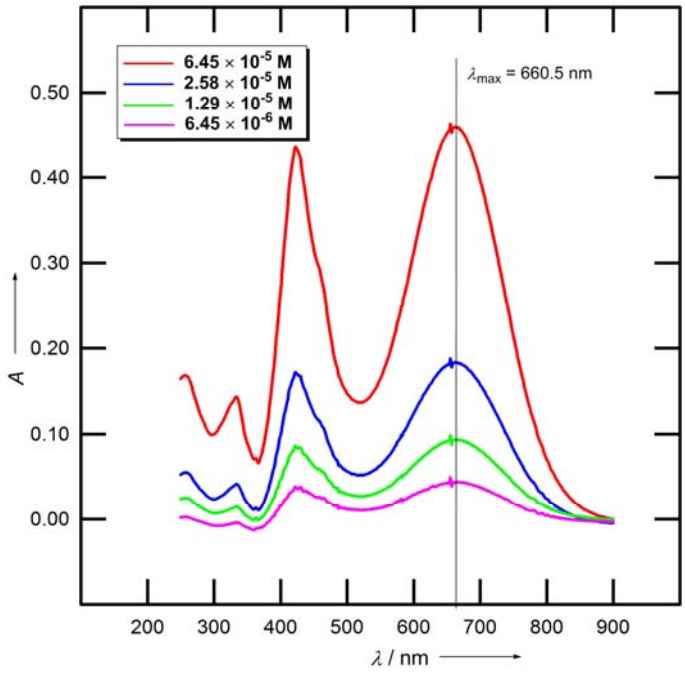

UV/Vis spectra of compound 6.

The spectra are listed in ascending order according to E_T^N values (see Table 1, main text).

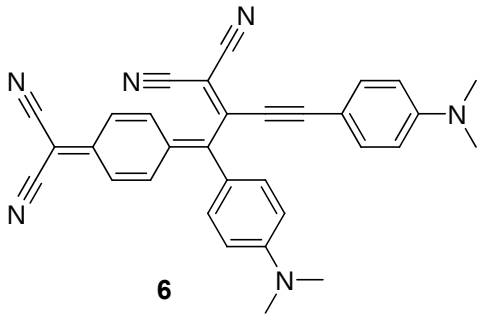

6

Figure 26SI. UV/VIS spectra of compound **6** in selected solvents (part 1).

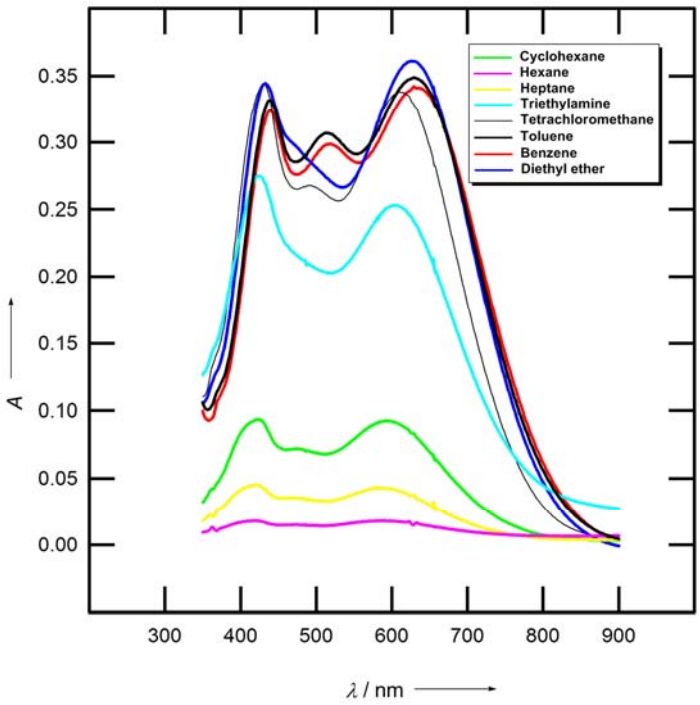

Figure 27SI. UV/VIS spectra of compound **6** in selected solvents (part 2).

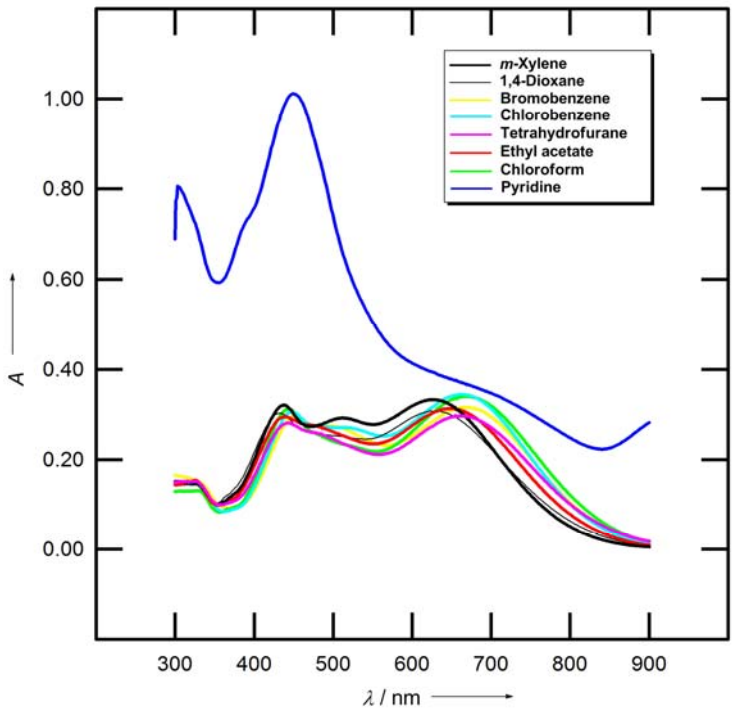

Figure 28SI. UV/VIS spectra of compound **6** in selected solvents (part 3).

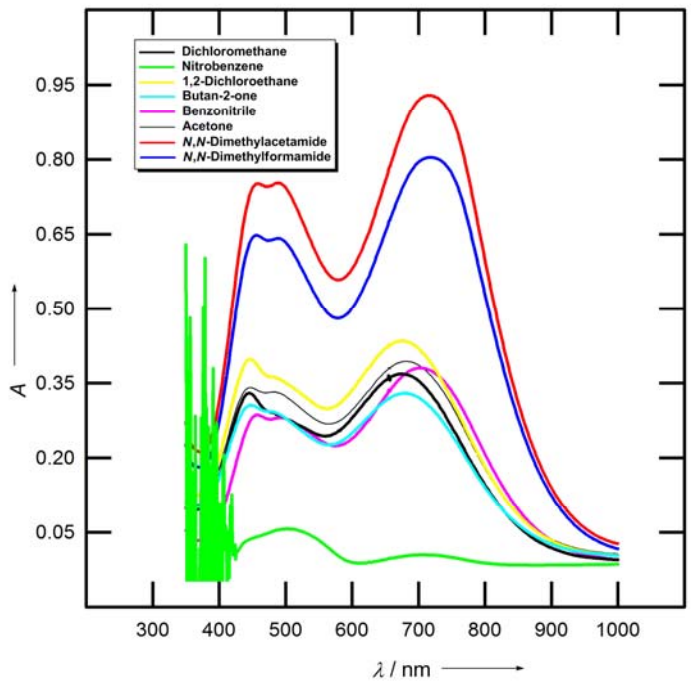

Figure 29SI. UV/VIS spectra of compound **6** in selected solvents (part 4).

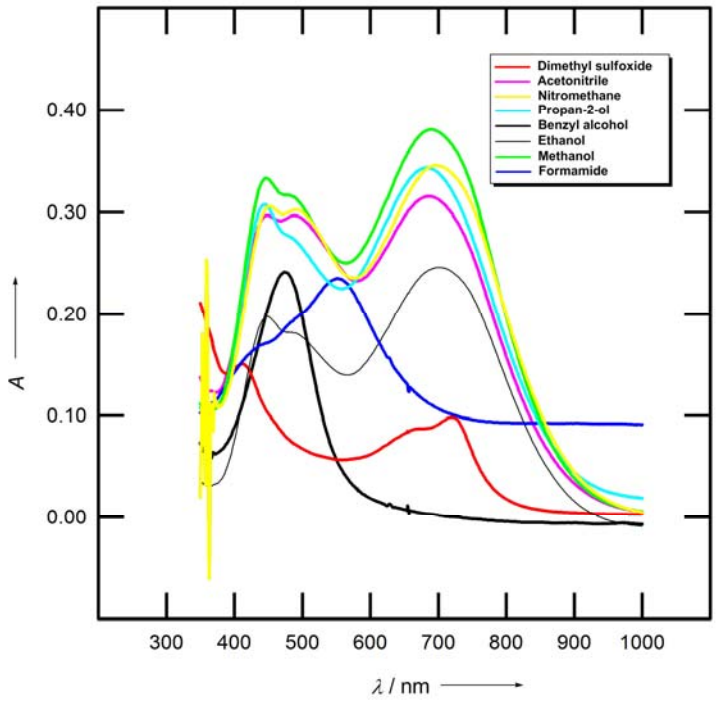

Figure 30SI. UV/VIS spectra of compound **7** in CH_2Cl_2 – concentration dependence.

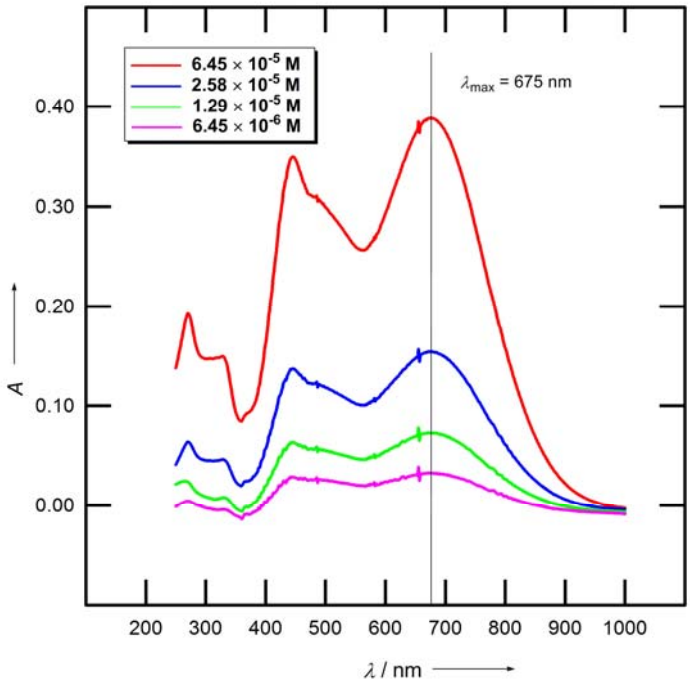

UV/Vis spectra of compound 7.

The spectra are listed in ascending order according to E_T^N values (see Table 1, main text).

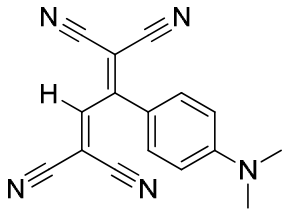

7

Figure 31SI. UV/VIS spectra of compound **7** in selected solvents (part 1).

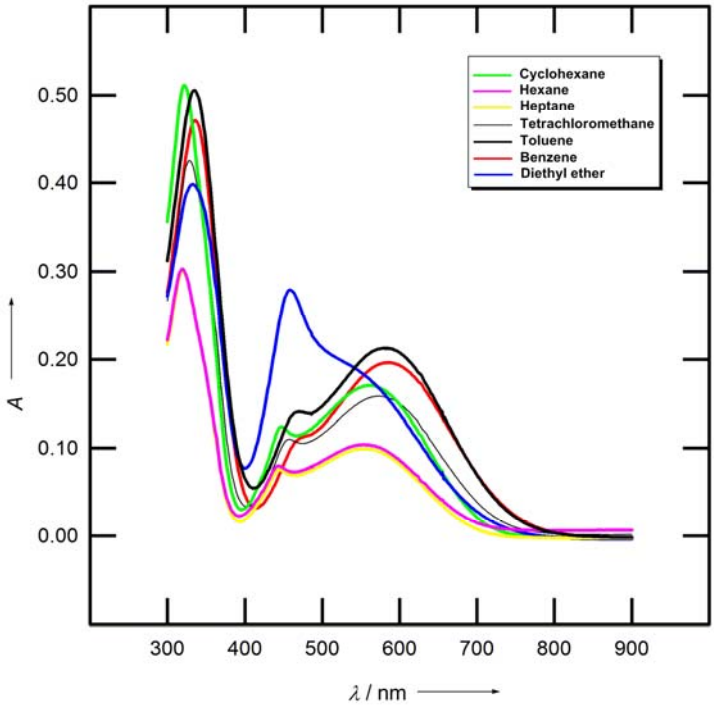

Figure 32SI. UV/VIS spectra of compound **7** in selected solvents (part 2).

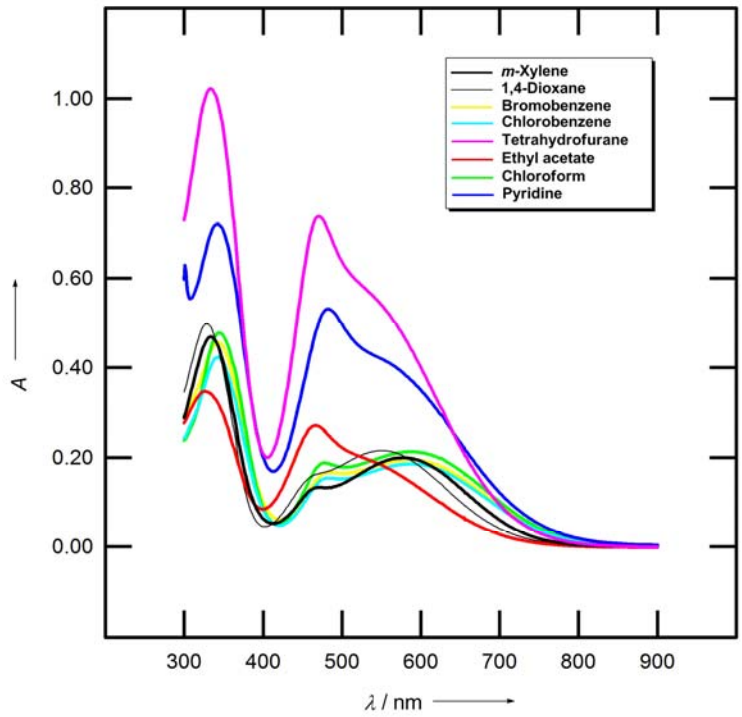

Figure 33SI. UV/VIS spectra of compound **7** in selected solvents (part 3).

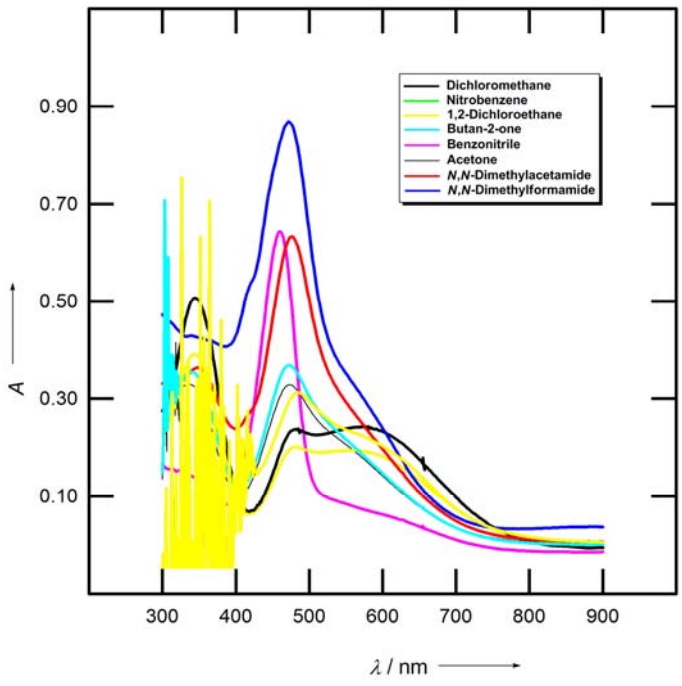

Figure 34SI. UV/VIS spectra of compound **7** in selected solvents (part 4).

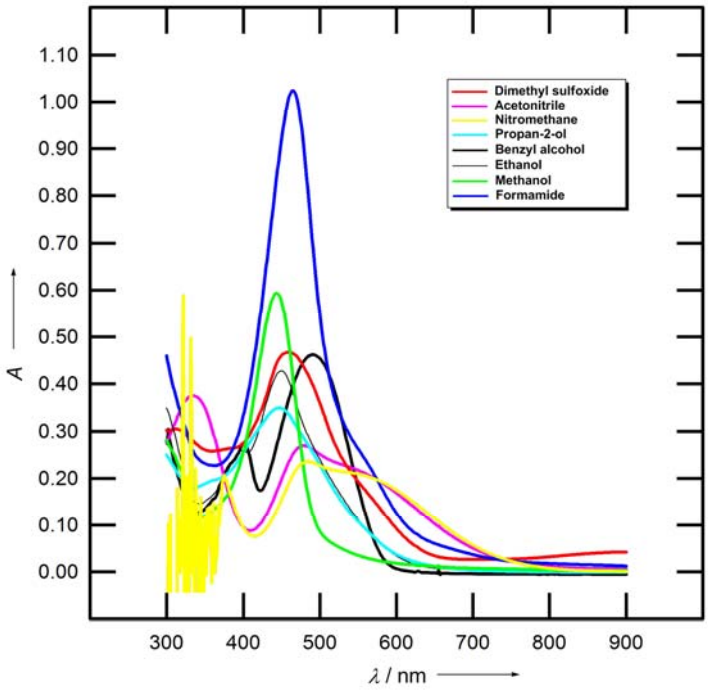

Figure 35SI. UV/VIS spectra of compound **7** in CH_2Cl_2 – dependence on concentration.

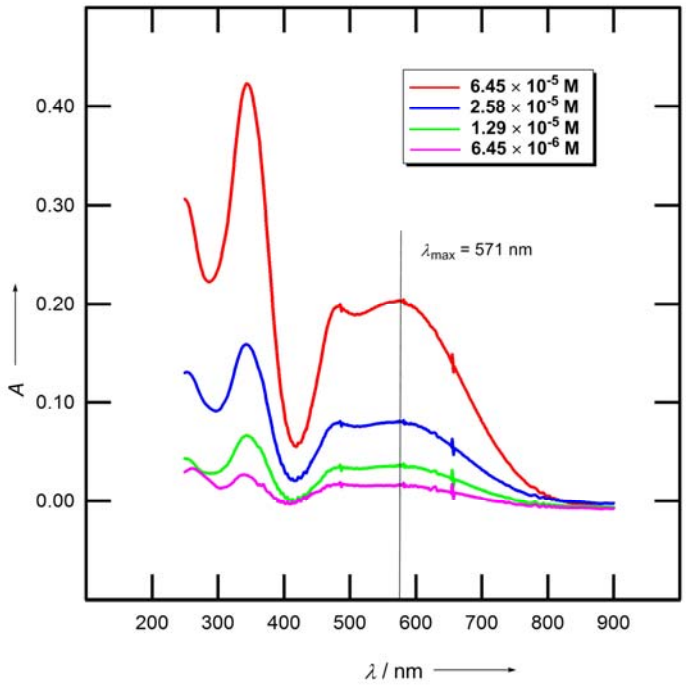

UV/Vis spectra of compound 8.

The spectra are listed in ascending order according to E_T^N values (see Table 1, main text).

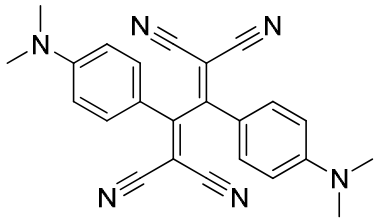

8

Figure 36SI. UV/VIS spectra of compound **8** in selected solvents (part 1).

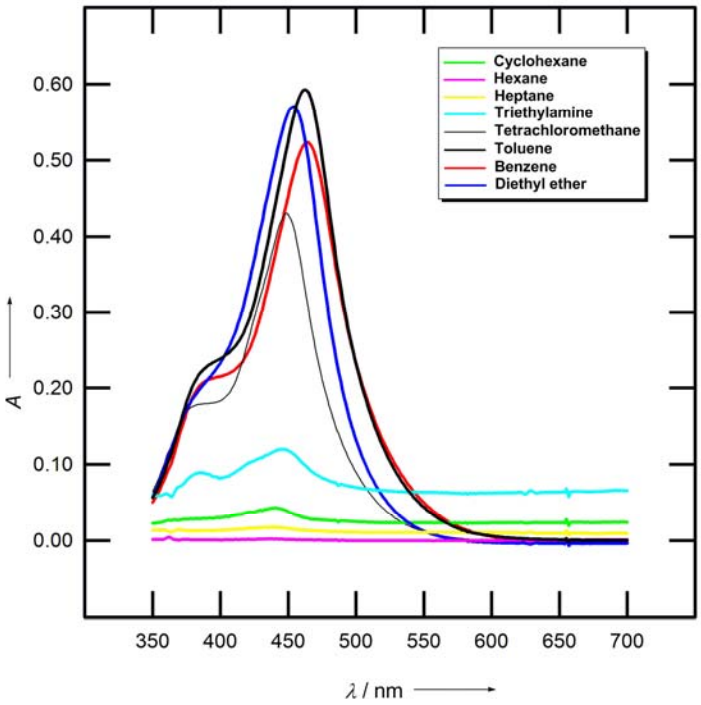

Figure 37SI. UV/VIS spectra of compound **8** in selected solvents (part 2).

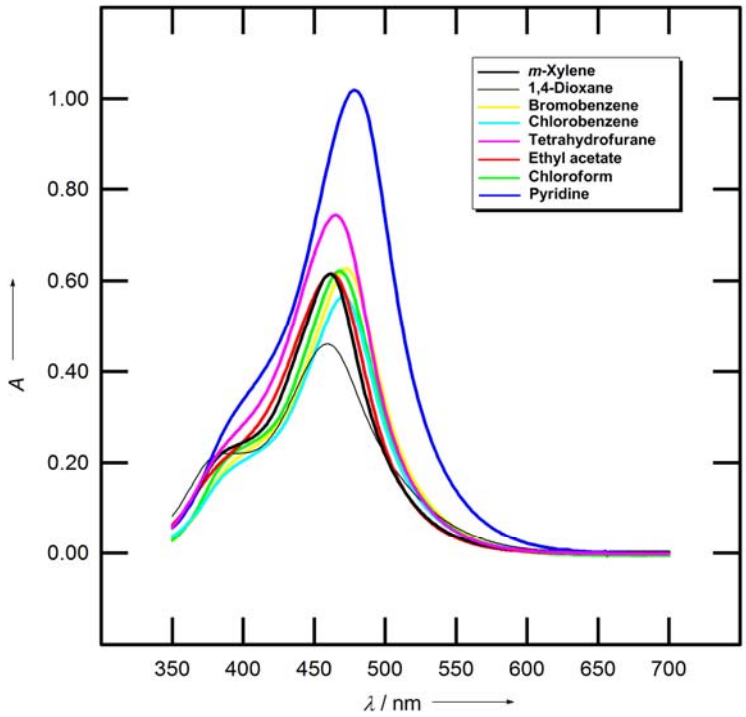

Figure 38SI. UV/VIS spectra of compound **8** in selected solvents (part 3).

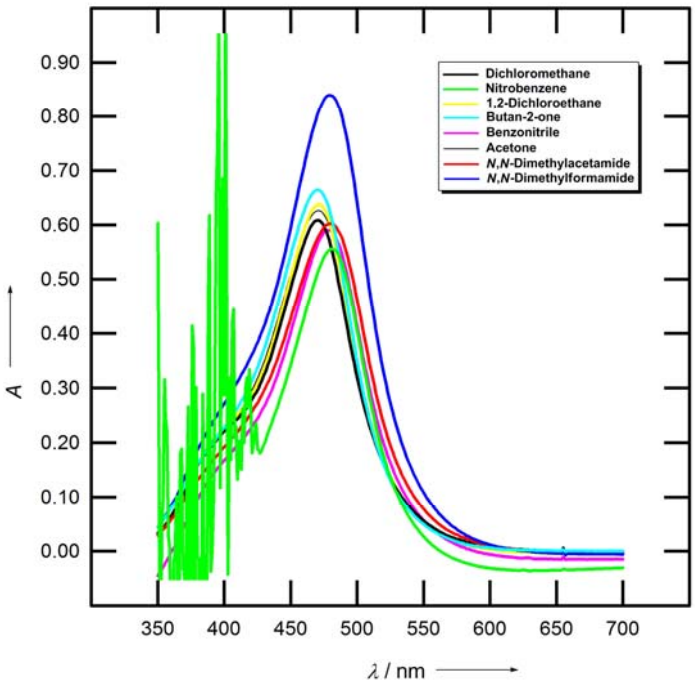

Figure 39SI. UV/VIS spectra of compound **8** in selected solvents (part 4).

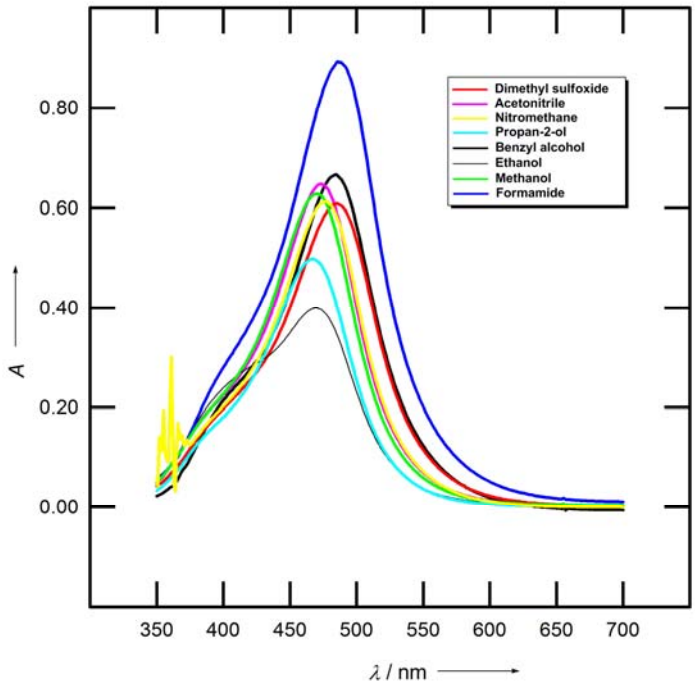

Figure 40SI. UV/VIS spectra of compound **8** in CH_2Cl_2 – dependence on concentration.

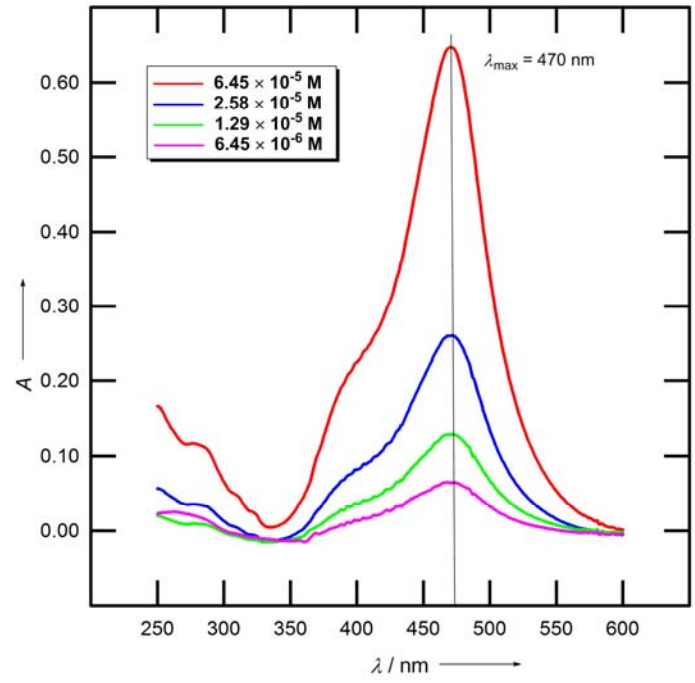

UV/Vis spectra of compound 9.

The spectra are listed in ascending order according to E_T^N values (see Table 1, main text).

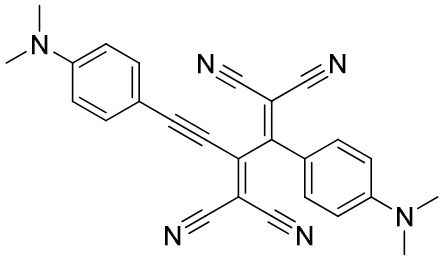

9

Figure 41SI. UV/VIS spectra of compound **9** in selected solvents (part 1).

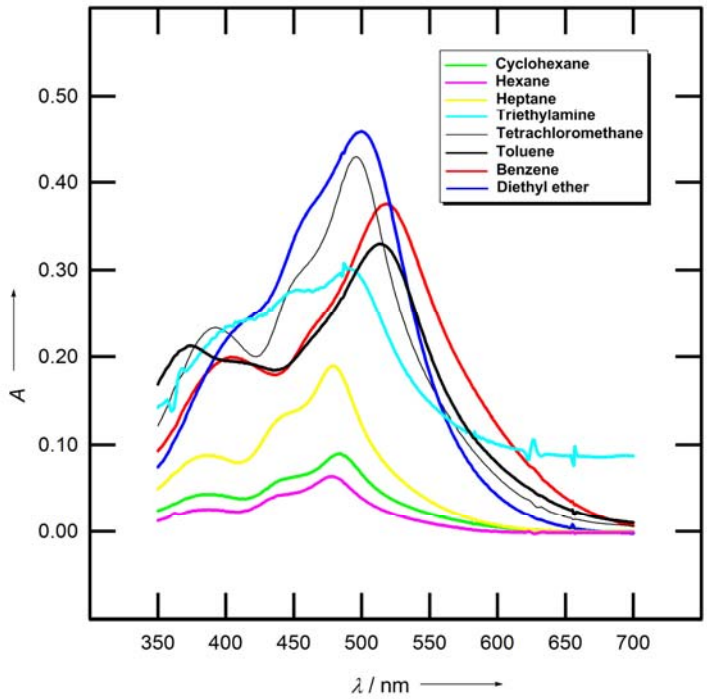

Figure 42SI. UV/VIS spectra of compound **9** in selected solvents (part 2).

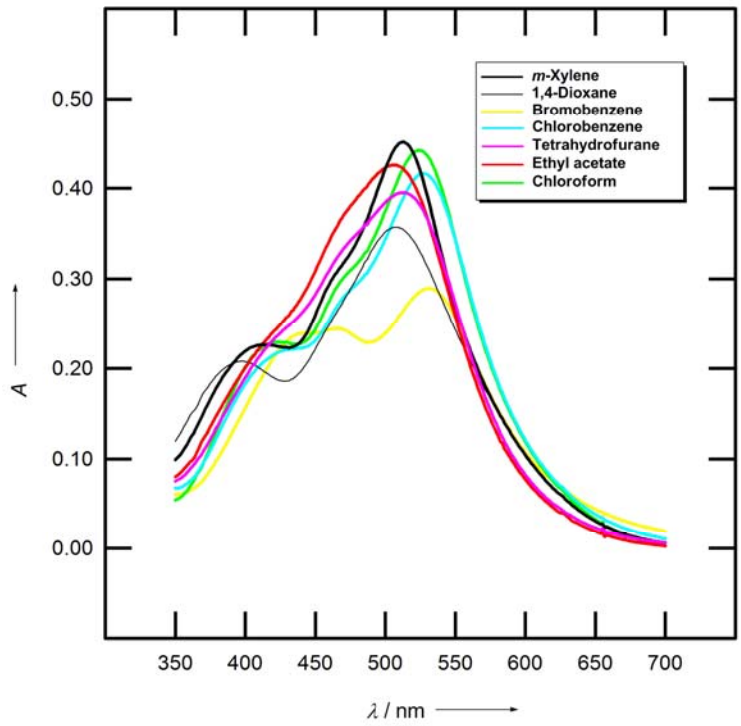

Figure 43SI. UV/VIS spectra of compound **9** in selected solvents (part 3).

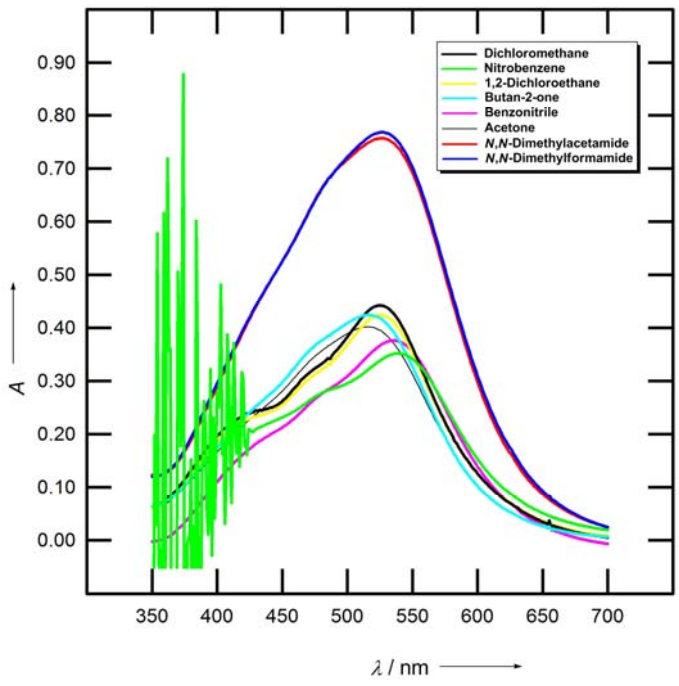

Figure 44SI. UV/VIS spectra of compound **9** in selected solvents (part 4).

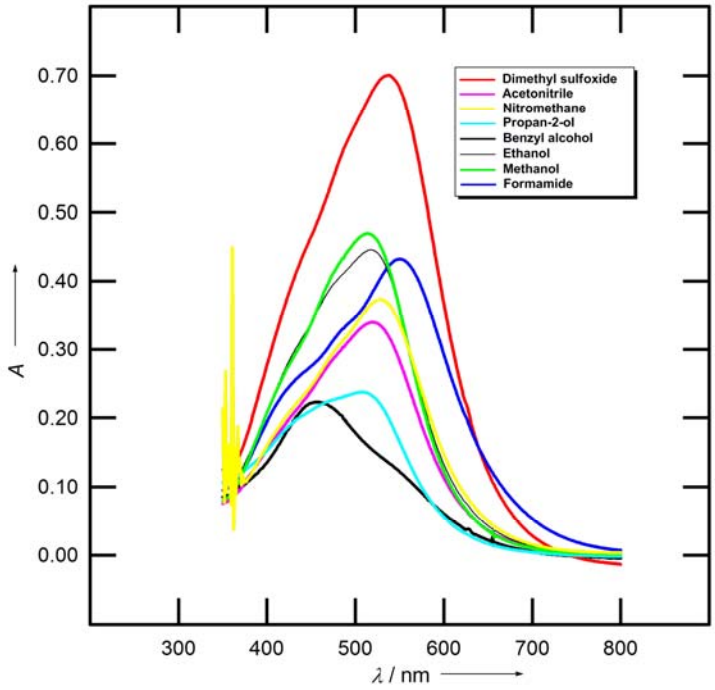

Figure 45SI. UV/VIS spectra of compound **9** in CH_2Cl_2 – dependence on concentration.

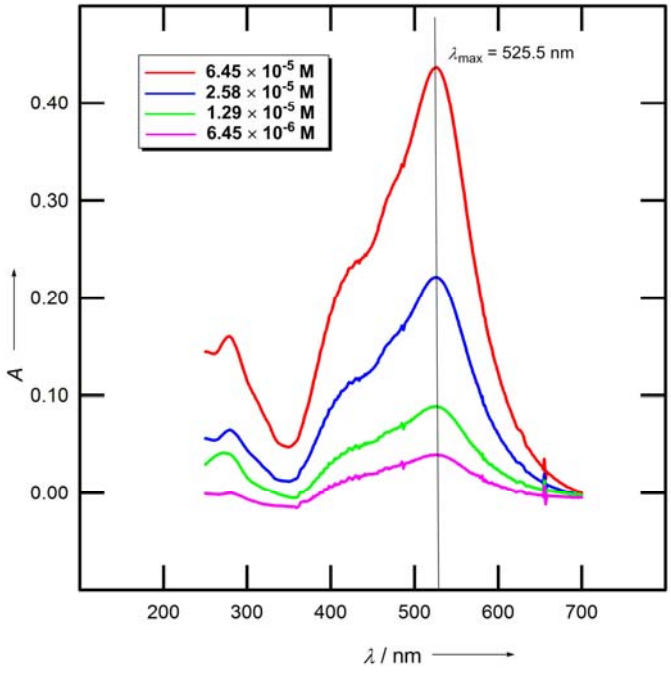

Solutions of the synthesized compounds

Figure 46SI. Colour of solutions of compounds **1**-**9**, dissolved in ***dichloromethane***.

Figure 47SI. Colour of solutions of compounds **1**-**9**, dissolved in ***N,N-dimethylacetamide***.